



1  
2  
3  
4  
5  
6  
7  
8  
9  
10  
11  
12  
13  
14  
15  
16  
17  
18  
19  
20  
21  
22  
23  
24  
25  
26

# **Do pelagic grazers benefit from sea ice?**

## **Insights from the Antarctic sea ice proxy IPSO<sub>25</sub>**

Katrin Schmidt<sup>1</sup>, Thomas A. Brown<sup>1,2</sup>, Simon T. Belt<sup>1</sup>, Louise C. Ireland<sup>3</sup>, Kyle W.R. Taylor<sup>4</sup>, Sally E. Thorpe<sup>3</sup>, Peter Ward<sup>3</sup>, Angus Atkinson<sup>5</sup>

<sup>1</sup>School of Geography, Earth and Environmental Sciences, University of Plymouth, Drake Circus, Plymouth, UK

<sup>2</sup>Marine Ecology and Chemistry, Scottish Association for Marine Science, Oban, UK

<sup>3</sup>British Antarctic Survey, Natural Environment Research Council, High Cross, Madingley Road, Cambridge, UK

<sup>4</sup>Elementar UK Ltd, Isoprime House, Earl Road, Cheadle Hulme, Stockport, UK

<sup>5</sup>Plymouth Marine Laboratory, Prospect Place, The Hoe, Plymouth, UK

Corresponding author: Katrin Schmidt (e-mail: [katrin.schmidt@plymouth.ac.uk](mailto:katrin.schmidt@plymouth.ac.uk))



## 27 ABSTRACT

28 Sea ice affects primary production in polar regions in multiple ways. It can dampen water column  
29 productivity by reducing light or nutrient supply, it provides a habitat for ice algae and on its seasonal  
30 retreat can condition the marginal ice zone (MIZ) for phytoplankton blooms. The relative importance of  
31 three different carbon sources (ice-derived, ice-conditioned, non-ice associated) for the polar food web  
32 is not well understood, partly due to the lack of methods that enable their unambiguous distinction. Here  
33 we analysed two highly branched isoprenoid (HBI) biomarkers to trace ice-derived and ice-conditioned  
34 carbon in Antarctic krill (*Euphausia superba*), and relate their concentrations to the grazers' body  
35 reserves, growth and recruitment. During our sampling in January/February 2003, the proxy for sea ice  
36 diatoms (a di-unsaturated HBI termed IPSO<sub>25</sub>,  $\delta^{13}\text{C} = -12.5 \pm 3.3\text{‰}$ ) occurred in open waters of the  
37 western Scotia Sea, where seasonal ice retreat was slow. In suspended matter, IPSO<sub>25</sub> was present at a  
38 few stations close to the ice edge, but in krill the marker was widespread. Even at stations that had been  
39 ice-free for several weeks, IPSO<sub>25</sub> was found in krill stomachs, suggesting that they gathered the ice-  
40 derived algae from below the upper mixed layer. Peak abundances of the proxy for MIZ diatoms (a tri-  
41 unsaturated HBI termed HBI III,  $\delta^{13}\text{C} = -42.2 \pm 2.4\text{‰}$ ) occurred in regions of fast sea ice retreat and  
42 persistent salinity-driven stratification in the eastern Scotia Sea. Krill sampled in the area defined by the  
43 ice edge bloom likewise contained high amounts of HBI III. As indicators for the grazer's performance  
44 we used the mass-length ratio, size of digestive gland and growth rate for krill, and recruitment for the  
45 biomass-dominant calanoid copepods *Calanoides acutus* and *Calanus propinquus*. These indices  
46 consistently point to blooms in the MIZ as an important feeding ground for pelagic grazers. Even  
47 though ice-conditioned blooms are of much shorter duration than the bloom downstream of the  
48 permanently sea ice-free South Georgia, they enabled fast growth and offspring development. Our study  
49 shows two rarely considered ways that pelagic grazers may benefit from sea ice: Firstly, after their  
50 release from sea ice, suspended or sinking ice algae can supplement the grazers' diet if phytoplankton  
51 concentrations are low. Secondly, conditioning effects of seasonal sea ice can promote pelagic primary  
52 production and therefore food availability in spring and summer.

53

54

55

56

57



## 58 1. Introduction

59 Over the last four decades, sea ice has shown a rapid decline in areal coverage in the Arctic and  
60 parts of the Antarctic (e.g. Bellingshausen- and Amundsen Seas). Here sea ice concentrations decrease  
61 during both summer (-10 to -13% per decade) and winter (-2% per decade) (Meier et al. 2017,  
62 Stammerjohn and Maksym 2017), and current trends towards later autumn sea ice advance and earlier  
63 spring sea ice retreat are likely to continue in both hemispheres (Stammerjohn et al. 2012). Ecosystem  
64 responses to the loss in sea ice and co-occurring warming and freshening include changes in primary  
65 productivity, alterations in phytoplankton community structure, range shifts for zooplankton, benthic  
66 organisms and fish, and decline in sea ice-dependent sea birds and mammals (Ducklow et al. 2007, Li et  
67 al. 2009, Grebmeier et al. 2010, Constable et al. 2014). Understanding such climate-related changes in  
68 structure and functioning of the polar ecosystem is imperative for the management of their resource  
69 exploitation (Smetacek and Nicol 2005).

70 Extended open-water seasons have been suggested to lead to higher primary production in the polar  
71 oceans (Arrigo and Thomas 2004, Arrigo 2017) and generate a negative feedback to climate change  
72 (Peck et al. 2010, Barnes and Tarling 2017). Some satellite-derived chlorophyll *a* -time series support  
73 this prediction (Arrigo et al. 2008), while others do not (Marchese et al. 2017). Along the Western  
74 Antarctic Peninsula, warming and a reduction in sea ice extent between 1978 and 2006 led to two very  
75 different scenarios (Montes-Hugo et al. 2009). In the southern part, perennial sea ice was replaced by  
76 seasonal sea ice and the ice-free summer days translated into more favourable conditions for  
77 phytoplankton growth (e.g. increased light). In contrast, in the northern part, loss of seasonal sea ice  
78 allowed a deepening of the upper mixed layer with less favourable light conditions for phytoplankton  
79 (Montes-Hugo et al. 2009). These observations illustrate the opposing effects that permanent- and  
80 seasonal sea ice can have on primary productivity. Thus, while the former prevents phytoplankton  
81 blooms, the latter can promote them. During seasonal ice retreat, meltwater can stabilize the surface  
82 layer and therefore enhance mean irradiance levels (Smith and Nelson 1986). Moreover, the release of  
83 trace elements from sea ice can alleviate nutrient limitation (Lannuzel et al. 2010, Schallenberg et al.  
84 2015). This explains why the MIZ is, on average, more productive than the permanently open waters of  
85 the Southern Ocean (Smith and Nelson 1986, Tréguer and Jacques 1992).

86 Chlorophyll *a* concentrations in sea ice are not accessible to satellite observations and therefore  
87 primary production estimates rely on sparse *in situ* measurements and numerical models. Such data  
88 suggest that primary production in sea ice accounts for only small amounts of total annual production in



89 polar waters; typically 2-10% in the Arctic and ca. 1-3% in the Southern Ocean south of 50°S (Arrigo  
90 2017). However, an important difference between phytoplankton and ice algae is that while the former  
91 is deeply mixed in the water column, sea ice provides a platform that retains the latter in the surface  
92 ocean where light levels can be sufficient for photosynthesis and net growth even during the dark  
93 season (Kottmeier and Sullivan 1987, Roukaerts et al. 2016). Therefore, ice algae supply an important  
94 autumn, winter and early spring carbon source to in-ice fauna, with subsequent transfer to the wider  
95 food web of ice-associated invertebrates, fish, seabirds and mammals (Ainley et al. 2017, Bluhm et al.  
96 2017, Caron et al. 2017, Bester et al. 2017). Other merits of ice algae are their enrichment in  
97 polyunsaturated fatty acids that make them a high-quality food source (Søreide et al. 2010, Wang et al.  
98 2014), while their tendency to aggregate and sink after being released from sea ice can be an important  
99 pathway of carbon export to the benthos (Riebesell et al. 1991, Renaud et al. 2007). Thus, the small  
100 contribution of ice algae to the overall primary production in the polar regions likely understates their  
101 ecological importance.

102 Dominant polar grazers such as calanoid copepods and euphausiids are adapted to the strong  
103 seasonality in primary production and the dynamic interface between ice and water (Smetacek and  
104 Nicol 2005). Postlarval stages of these species biosynthesise large lipid stores which enable them to  
105 survive long periods without food (Hagen and Auel 2001). Some species remain active during winter  
106 (e.g. the Antarctic copepod *Calanus propinquus* and the krill *Euphausia superba*) and can be found  
107 under sea ice feeding on ice algae or heterotrophs, if available (Atkinson and Shreeve 1995, Flores et al.  
108 2012a, Schmidt et al. 2014). In other species, e.g. the Arctic *Calanus hyperboreus* and *C. glacialis*  
109 together with the Antarctic *Calanoides acutus*, the life cycle is closely coupled to the bloom period:  
110 they overwinter at depth in dormancy, are able to fuel their gonad maturation from lipid reserves and  
111 their offspring make the most of the brief productive season (Hagen and Auel 2001). However, years  
112 with very early or very late ice retreat can lead to poor population development of these species (Quetin  
113 and Ross 2003, Ward et al. 2006, Leu et al. 2011). Optimal conditions are reached when peak times of  
114 food demand and food availability are tightly matched (Quetin and Ross 2003, Søreide et al. 2010). A  
115 change towards earlier sea ice retreat has been suggested to cause severe mismatches (Søreide et al.  
116 2010). Whether this has already impacted the populations of polar grazers is largely unknown, however,  
117 due to the paucity of adequate baseline data that allow us to distinguish interannual variability from  
118 long-term trends (Wassmann et al. 2011).

119 An exception is Antarctic krill that have been sampled extensively over the last 90 years due to their  
120 central role in Antarctic food webs and their commercial interest (Smetacek and Nicol 2005). The main



121 habitat of Antarctic krill is the south-west Atlantic Sector of the Southern Ocean (Atkinson et al. 2008),  
122 which largely overlaps with areas of negative trends in sea ice concentrations (western Antarctic  
123 Peninsula, north-west Weddell Sea) (Stammerjohn and Maksym 2017). A long-term data set shows that  
124 krill stocks in this region have significantly declined (Atkinson et al. 2014), with consequences for  
125 populations of krill predators such as penguins and seals (Reid and Croxall 2001, Fraser and Hoffmann  
126 2003, Trivelpiece et al. 2011, Forcada and Hoffmann 2014). Concurrent expansion and operational  
127 changes in Antarctic krill fisheries (Kawaguchi et al. 2009) make the krill decline a significant issue of  
128 Southern Ocean ecosystem management (Flores et al. 2012b). However, the key mechanism linking  
129 krill and sea ice remains elusive (Meyer et al. 2017). Some studies stress the crucial role of sea ice for  
130 overwinter survival of krill larvae by providing food and shelter (Daly 2004, Meyer et al. 2009,  
131 Kohlbach et al. 2017), while others point to sea ice as an important habitat for juvenile and adult krill  
132 during spring and summer (Marschall 1988, Brierley et al. 2002, Flores et al. 2012a) or emphasize  
133 indirect effects of seasonal ice cover due to its control on summer phytoplankton productivity and  
134 therefore krill recruitment (Quetin and Ross 2003, Saba et al. 2014).

135 To resolve some of this uncertainty it is essential to quantify the relative importance of sea ice-  
136 derived, ice-conditioned and non-ice associated carbon in krill diet, and to relate dietary differences to  
137 the performance of krill in terms of growth, recruitment and accumulation of body reserves. However,  
138 ice algae-produced carbon has rarely been traced through Southern Ocean food webs (Goutte et al.  
139 2013, Jia et al. 2016, Kohlbach et al. 2017), as distinguishing it unambiguously from phytoplankton-  
140 produced carbon is difficult. Here we tackle this challenge by measuring two highly branched  
141 isoprenoid (HBI) biomarkers, which are metabolites of certain diatom species and established proxies  
142 for palaeo sea ice reconstructions (Armand et al. 2017). Around Antarctica, mixtures of a di-unsaturated  
143 HBI (referred to as diene II in previous studies; see Fig. 1) and a tri-unsaturated HBI (referred to as  
144 triene III in previous studies, thereafter HBI III, Fig. 1) have repeatedly been found in sediment cores,  
145 water column samples and Antarctic predators (Massé et al. 2011, Collins et al. 2013, Goutte et al.  
146 2013, 2014a,b, Smik et al. 2016). The samples were obtained from the Atlantic-, Indian- and Pacific  
147 sector of the Southern Ocean, suggesting a widespread occurrence of these biomarkers. However, only  
148 diene II has been identified in sea ice samples, and its enrichment in  $^{13}\text{C}$  ( $\delta^{13}\text{C} = -5.7$  to  $-17.8\text{‰}$ ) is in  
149 line with a depleted dissolved inorganic carbon pool in the semi-enclosed sea ice matrix (Massé et al.  
150 2011). This has led to the name ‘Ice Proxy for the Southern Ocean with 25 carbon atoms’ – IPSO<sub>25</sub>,  
151 with the sympagic diatom *Berkeleya adeliensis* being recently identified as one of the source species  
152 (Belt et al. 2016). In contrast, HBI III is produced by certain pelagic diatom species, e.g. *Rhizosolenia*



153 spp. (Belt et al. 2017), and its significantly lighter stable isotopic signature ( $\delta^{13}\text{C} = -35.0$  to  $-41.6\text{‰}$ )  
154 indicates a replete carbon pool typical for open waters (Massé et al. 2011). Previous water column and  
155 sediment studies have shown relative enhancements in HBI III within the MIZ in the Arctic and  
156 Antarctic (Collins et al. 2013, Etourneau et al. 2013, Belt et al. 2015, Smik et al. 2016, Ribeiro et al.  
157 2017), even when other productivity signatures were less revealing, possibly reflecting a preferred  
158 habitat for the HBI III-producing species within this setting (Belt et al. 2015). As such, measurements of  
159 these two HBIs provide an opportunity to distinguish between direct and indirect effects of sea ice:  
160 IPSO<sub>25</sub> indicates ice algae-produced carbon, while HBI III indicates phytoplankton-produced carbon in  
161 waters conditioned by sea ice (i.e. the MIZ). Importantly, both IPSO<sub>25</sub> and HBI III have been identified  
162 in body tissues of seabirds, seals and fish, which confirms their transfer across Antarctic food webs and  
163 supports their use as trophic markers (Goutte et al. 2013, 2014a,b). However, detailed interpretation of  
164 these biomarkers still lacks basic knowledge about (1) the oceanographic conditions (e.g. sea ice  
165 history, stratification, mixed layer depth, chl *a* concentration) that favour the abundance of IPSO<sub>25</sub> and  
166 HBI III-producing diatoms; (2) the subsequent uptake and turnover of IPSO<sub>25</sub> and HBI III by Antarctic  
167 grazers; and (3) the link between the ingested carbon-source and the performance of the grazers.

168 In this study, we contribute to the development of the HBI-based approach by analysing Antarctic  
169 krill and suspended material during seasonal sea ice retreat in the Scotia Sea (Atlantic Sector of the  
170 Southern Ocean) in January-February 2003. The suitability of different feeding grounds (MIZ,  
171 permanently ice-free Scotia Sea, South Georgia) for pelagic grazers was established based on the mass-  
172 length ratio, size of digestive gland and growth rate of krill, and recruitment of the biomass-dominant  
173 calanoid copepods *Calanoides acutus* and *Calanus propinquus*.

174

## 175 2. Methods

### 176 2.1 Phytoplankton bloom development

177 Chlorophyll *a* (chl *a*) concentrations were obtained from ocean colour radiometry (MODIS, 9 km  
178 standard product, 8-day composites, 6th of September – 30th of March, 2002-2015). The Scotia Sea  
179 (55-63°S, 25-60°W) and South Georgia region (52-55°S, 32-42°W) were divided into subareas of 1°Lat  
180 by 2.5°Lon. For each of these subareas the monthly- and annual mean chl *a* concentration and the  
181 annual bloom duration (number of weeks with chl *a*  $\geq 0.5 \text{ mg m}^{-3}$ ) were determined for the 2002/2003  
182 season and compared to the longer-term average, 2002-2015.

183  
184



## 185 2.2 Oceanography

186 Shipboard data were collected from the research vessel RRS ‘James Clark Ross’ cruise JR82  
187 between 9 January and 16 February 2003. Fifty-five hydrographic stations were positioned at 110 km  
188 intervals along 8 transects across the Scotia Sea, commencing north of Elephant Island and traversing  
189 eastward. A further 6 stations were located to the north-west of South Georgia (Fig. 2). At each station,  
190 vertical profiles of conductivity-temperature-depth (CTD) and blue light-stimulated chlorophyll  
191 fluorescence were collected with a SeaBird 911+CTD and attached Aqua-Tracka Mk III fluorometer  
192 (Chelsea Instruments) (Korb et al. 2005). Mixed-layer depths were calculated as the depth where the  
193 density difference ( $\Delta\sigma$ ) relative to the surface water is  $0.05 \text{ kg m}^{-3}$  (Venables et al. 2013). Size  
194 fractionated chl *a* was measured from water samples collected at 20 m depth. Samples were filtered  
195 sequentially onto a series of 12, 2 and  $0.2 \mu\text{m}$  polycarbonate membrane filters ( $\varnothing 47 \text{ mm}$ ), and analysed  
196 for chl *a* after extraction in 90% acetone (Korb et al. 2005).

197

## 198 2.3 Sea ice cover

199 Monthly sea ice edges were calculated using sea ice concentrations from Nimbus-7 SMMR and  
200 DMSP SSM/I-SSMIS passive microwave data. Monthly composites were calculated using the median  
201 of the daily grids for each month. These were then contoured at 15% to extract a line indicating average  
202 position of the sea ice edge for each month. Timelines of sea ice over at each of our sampling stations  
203 were established within a 50km radius. Using these zones, we extracted an average value of sea ice  
204 concentration on a daily basis. The input data was derived from Microwave Scanning Radiometer-Earth  
205 Observation System (AMSR-E) aboard the NASA’s Aqua satellite and the Defense Meteorological  
206 Satellite Program SSM/I, which is at a higher spatial resolution of 6.25km. Further detail in Cavalieri et  
207 al. (1996) and Spreen et al. (2008).

208

## 209 2.4 Sampling of suspended matter, krill and faecal pellets

210 Suspended matter was sampled from the ship’s non-toxic seawater supply located ~6 m below the  
211 sea surface. Seawater samples (3 L) were filtered onto pre-ashed GF/F filters and stored at  $-80^\circ\text{C}$  until  
212 analysis. Krill swarms were identified in the vicinity of each station using a Simrad EK60 echosounder  
213 and sampled with a Rectangular Midwater Trawl (RMT 8). The RMT was equipped with two nets that  
214 were opened and closed remotely from the ship, allowing short duration hauls targeted on specific krill  
215 schools in the upper 50 m of the water column. One sub-sample of the freshly caught krill was  
216 immediately frozen at  $-80^\circ\text{C}$  for subsequent analysis of HBIs. Another sub-sample of krill was kept



217 alive to allow for defecation. These krill were placed into buckets filled with surface water and pellets  
218 were collected as soon as visible on the bottom of the buckets. The pellets were transferred into 1 ml  
219 Eppendorf tubes and rinsed repeatedly with GF/F-filtered seawater with a final brief rinse in deionised  
220 water. The supernatant water was removed and vials were stored at -80°C.

221

### 222 *2.5 Krill dissections*

223 In the laboratory, krill body length was measured from the anterior edge of the eye to the tip of the  
224 telson. Three to fifteen individuals of the same body length were selected for HBI analysis. If available,  
225 up to six different size classes were analysed per station and krill were dissected into stomach content,  
226 gut, digestive gland, third abdominal segment (muscle) and remaining body. A pooled sample of each  
227 of these components was placed in a pre-weighed vial, freeze-dried for 24 h and re-weighed on a  
228 Sartorius microbalance. The mass of the digestive gland was related to the total body mass.

229

### 230 *2.6 HBI extraction and analysis*

231 HBIs were extracted and analysed as described previously for filtered water samples and  
232 zooplankton tissue (Brown and Belt 2012, Smik et al. 2016, Belt et al. 2016). In brief, freeze-dried  
233 faecal pellets and krill body fractions were ground using a pestle and mortar. Following addition of an  
234 internal standard [9-octyl-8-heptadecene (10 µl; 2 µg ml<sup>-1</sup>)] to facilitate HBI quantification, samples  
235 were saponified with 5% KOH (filters) or 20% KOH (krill tissue) (70°C; 60 min). Thereafter, non-  
236 saponifiable lipids were extracted with hexane (3 x 1 ml) and purified by open column chromatography  
237 (SiO<sub>2</sub>). HBIs were eluted using hexane (5 column volumes) before being dried (N<sub>2</sub> stream, 25°C). The  
238 analysis of partially purified non-polar lipids containing IPSO<sub>25</sub> and triene III was carried out using an  
239 Agilent 7890A gas chromatograph, coupled to an Agilent 5975 mass selective detector, fitted with an  
240 Agilent HP-5ms column with auto-splitless injection and helium carrier gas. Identification of individual  
241 lipids was achieved by comparison of their retention index and mass spectrum with those obtained from  
242 purified standards. Quantification of IPSO<sub>25</sub> and HBI III was achieved by integrating individual ion  
243 (IPSO<sub>25</sub>: *m/z* 348.3; HBI III: *m/z* 346.3) responses in single-ion monitoring mode, and normalising these  
244 to the corresponding peak area of the internal standard and an instrumental response factor obtained  
245 from purified standards (Belt et al. 2012). The GC-MS-derived masses of both HBIs were converted to  
246 water column concentrations using the volume of filtered water, and to concentrations in krill body  
247 fractions using the mass of the sample extracted. For simplicity in representing biomarker ratios, we use



248 the terms I and H for IPSO<sub>25</sub> and HBI III, respectively. Thus, the proportion of IPSO<sub>25</sub> to the combined  
249 concentration of IPSO<sub>25</sub> and HBI III is given by  $I/(I+H)$ .

250

### 251 *2.7 Stable isotope determination*

252 The stable carbon isotopic compositions ( $\delta^{13}\text{C}$ ) of IPSO<sub>25</sub> and HBI III were determined by gas  
253 chromatography–isotope ratio mass spectrometry (GC–IRMS), using an IsoPrime100 IRMS with GC5  
254 interface and Agilent 7890B GC installed with an Agilent HP-5MS column (30 m × 0.2 mm I.D., film  
255 thickness 0.25  $\mu\text{m}$ ). Samples in ca. 10–150  $\mu\text{l}$  hexane were injected in splitless mode with the following  
256 inlet conditions: 250°C, purge flow 25 ml min<sup>-1</sup>, purge time 0.75 min. GC carrier gas (He) flow rate was  
257 1 mL min<sup>-1</sup>, oven program as follows: 1 minute hold at 50°C, ramp to 310°C at 10°C min<sup>-1</sup>, then 13  
258 minute hold. The combustion furnace consisted of a 0.7 mm I.D. quartz tube packed with CuO pellets,  
259 held at 850°C. GC–IRMS data were calibrated using the certified Indiana alkane standard mix A5  
260 (Indiana University, Bloomington, IN, USA) and all results reported in delta notation ( $\delta^{13}\text{C}$ ) relative to  
261 VPDB. IPSO<sub>25</sub> and HBI III were identified in GC–IRMS chromatograms by retention time comparison  
262 with corresponding GC–MS analyses. IonOS software (Elementar UK Ltd) was used to process GC–  
263 IRMS data; ‘Peak Mapping’ functionality was used to designate specific compound identifications  
264 across multiple injections. The A5 alkane mix was analysed in at least duplicate, and calibrations were  
265 constructed from at least three interspersed replicate measurements of the A5 mix. Reproducibility of all  
266 individual alkanes was always  $\leq 0.35$  ‰. Root mean standard error (RMSE) of each of the calibrations  
267 was usually  $\leq 0.25$  ‰, with an overall RMSE for all calibrations combined of  $\leq 0.21$  ‰, reflecting both  
268 the reliability of each calibration, and the long-term stability of the system (analyses were undertaken  
269 over a three week period in total). Samples containing IPSO<sub>25</sub> and HBI III were run in triplicate;  
270 precisions for both compounds were  $\leq 0.27$  (see Table 1).

271

### 272 *2.8 Copepod abundance and stage composition*

273 Copepods were collected at each station with a motion-compensating Bongo net of 200  $\mu\text{m}$  mesh  
274 size. The net was deployed to 400 m and hauled vertically back to the surface. The content of the net  
275 was preserved in 10% (v:v) formalin in seawater. In the laboratory, samples were divided into  
276 appropriate aliquots with a Folsom plankton splitter and examined under a binocular microscope.  
277 *Calanoides acutus* and *Calanus propinquus* were identified to their copepodite stages (stage I to VI).  
278 The mean age of the population was calculated as the sum of the products of each stage number and its  
279 abundance, divided by the total abundance.



### 280 3. Results

#### 281 3.1 Development of the Scotia Sea phytoplankton bloom in 2002/2003

282 In October 2002, elevated chl *a* concentrations ( $>0.5 \text{ mg m}^{-3}$ ) were only found north of South  
283 Georgia ( $\sim 53^\circ\text{S}$ ), and one month later in the north-eastern Scotia Sea ( $\sim 56^\circ\text{S}$ , Fig. 3A). With the rapid  
284 retreat of sea ice in December 2002, the bloom in the east extended south and reached the northern  
285 Weddell Sea in January 2003 ( $\sim 62^\circ\text{S}$ , Fig. 3B). In February 2003, chl *a* concentrations remained high in  
286 the eastern Scotia Sea and at South Georgia, but started to decline in March except for a local peak at  
287 the southern edge of our study area ( $\sim 63^\circ\text{S}$ , Fig. 3C). In the western and central Scotia Sea, chl *a*  
288 concentrations remained low throughout the summer, apart from slightly enhanced values across the  
289 South Orkney Plateau in January 2003. Compared to the longer-term average (2002-2015), there was a  
290 negative anomaly in phytoplankton abundance in the central Scotia Sea in 2002/2003, but a surplus in  
291 the east (Fig. 3D, E). At the East Scotia Ridge, mean annual chl *a* concentrations were up to  $0.7 \text{ mg m}^{-3}$   
292 higher and the bloom lasted up to 16 weeks longer in 2002/2003 than in the 2002-2015 average (Fig.  
293 3E).

294

#### 295 3.2. Spatial distribution of oceanographic data and HBIs

296 During maximum sea ice extent the previous winter, about two-thirds of our sampling stations were  
297 ice covered (Fig. 4A). One month before the cruise, stations in the southern Scotia Sea were still ice  
298 covered by 50-75 % concentration (Fig. 4B), but values had dropped to  $< 6\%$  at the time of sampling.  
299 Surface temperatures ranged from  $-1.2^\circ\text{C}$  at stations near the ice edge to  $4.5^\circ\text{C}$  at South Georgia (Fig.  
300 4C). Surface salinity was likewise lowest near the retreating ice edge and highest within the Southern  
301 Antarctic Circumpolar Current Front (range: 33.1-34.4; Fig. 4D). Stations of the Scotia Sea that had  
302 been ice covered showed a stronger vertical density gradient and shallower mixed layer than northerly  
303 stations that remained ice free (Fig. 4E, F). Highest surface chl *a* concentrations in the eastern Scotia  
304 Sea and near South Georgia coincided with the dominance of large phytoplankton size classes (Fig.  
305 4G,H).

306 Out of the 61 stations where suspended matter was analysed for HBIs, 6 contained  $\text{IPSO}_{25}$  and 51  
307 HBI III (Fig. 5A, B). Stations where  $\text{IPSO}_{25}$  occurred in suspended matter were all located near the ice  
308 edge (Stn 6, 18, 19, 20, 31, 48), while stations with elevated HBI III concentrations were found near the  
309 ice edge (Stn 45, 46, 49-53) and further north (Stn 12, 25, 26, 37, 40). At stations where both HBIs co-  
310 occurred,  $\text{IPSO}_{25}$  concentrations usually exceeded those of HBI III [mean  $I/(I+H)$ :  $0.6 \pm 0.3$ ,  $n=6$ ; Fig.



311 5C]. In addition to suspended matter, krill from 47 stations were also analysed for HBIs. IPSO<sub>25</sub> was  
312 present in 21 of these, whereas HBI III was found in all 47 (Fig. 5D, E). The spatial distribution of  
313 IPSO<sub>25</sub> in krill matched that found in suspended matter, with highest concentrations near the ice edge.  
314 However, IPSO<sub>25</sub> could also be detected in krill at stations further north, even though it was not  
315 identified in suspended matter from the upper mixed layer. Highest HBI III concentrations in krill were  
316 observed in the central Scotia Sea (Stn 13, 14, 22) and in the east (Stn 47, 52, 54), which only partly  
317 overlaps with locations of highest HBI III concentrations in suspended matter. However, as for  
318 suspended matter, maximum HBI III concentrations in krill exceeded those of IPSO<sub>25</sub> by an order of  
319 magnitude (ca. 4300 vs 450 ng g<sup>-1</sup>), and highest I/(I+H) ratios occurred near the ice edge in the western–  
320 and central Scotia Sea [mean I/(I+H): 0.3±0.2, n=21; Fig. 5F].

321

### 322 3.3 The habitat of IPSO<sub>25</sub> vs. HBI III-producing diatoms

323 Highest IPSO<sub>25</sub> and HBI III concentrations in suspended matter were both found in the southern  
324 Scotia Sea near the retreating ice edge. However, the occurrence of IPSO<sub>25</sub> was restricted to the western  
325 and central Scotia Sea, while HBI III reached highest concentrations in the east (Fig. 5). The  
326 oceanographic conditions in those regions showed clear differences. At stations with high IPSO<sub>25</sub>  
327 concentrations (Stn 18, 19, 20, 31), ice cover had just retreated and re-appeared shortly after the stations  
328 were sampled (Fig. 6A). Sub-zero surface temperatures, a strong salinity gradient in the upper ~25 m  
329 water column, and relatively low chl *a* concentrations are in line with the recent sea ice melt (Fig. 6C-  
330 E). In contrast, the eastern stations with high HBI III concentrations (Stn 45, 50, 51, 52) had been ice-  
331 free for ~1 month at the time of sampling. Higher temperatures, higher surface salinity and elevated chl  
332 *a* concentrations suggest a progression of upper water column processes since the ice retreat (Fig. 6B-  
333 E).

334 To confirm the source environments of IPSO<sub>25</sub> and HBI III, we analysed their carbon isotopic  
335 signature after extraction from krill sampled at various locations. In each case, IPSO<sub>25</sub> had much higher  
336 δ<sup>13</sup>C values than HBI III (-12.5±3.2 ‰ vs -42.2±3.0‰; Table 1), and their respective values are  
337 consistent with those reported for the same lipids isolated from sea ice, phytoplankton and sediment  
338 (Massé et al. 2011, Belt et al. 2016).

339 In the south-eastern Scotia Sea, there was a large area where high HBI III concentrations coincided  
340 with elevated chl *a* concentrations and high proportions of large phytoplankton (Fig. 4G, H, Fig. 5B).  
341 Oceanographically, this area was characterised by a strong vertical gradient in temperature and salinity



342 (and therefore in water column density), and by shallow upper mixed layers (Fig. 4C-F, Fig. 7). A  
343 comparison of the stations' history of ice cover shows that the vertical density gradient was driven by  
344 ice melt. There was a highly significant linear relationship between density- and salinity gradients, with  
345 strongest density gradients at stations that had >30% ice cover one month before sampling (Fig. 8). In  
346 contrast, at more northerly stations that had been ice-free for longer, there was a mixed rather than  
347 stratified surface layer and chl *a* concentrations were much lower (Fig. 7). Only at South Georgia were  
348 surface temperatures high enough to co-influence the vertical density gradient.

349 In the western and central Scotia Sea, stations near the ice edge were also characterised by high  
350 density gradients and shallow mixed layers. However, here high HBI III concentrations were only found  
351 in krill (Fig. 5E, especially Stn 22), not in suspended matter (Fig. 4E-G, Fig. 5B).

352

#### 353 *3.4 IPSO<sub>25</sub> and HBI III concentrations in krill – the role of body fraction and body size*

354 The analysis of krill body fractions shows that not all of the ingested IPSO<sub>25</sub> and HBI III was  
355 absorbed into body tissue, but part remained in the intestine and was then egested via their faecal  
356 pellets. Thus, IPSO<sub>25</sub> and HBI III concentrations in the stomach were, on average, three times higher  
357 than in the digestive gland, over fifty-times higher than in the muscle, and about ten-times higher than  
358 in the whole krill (Table 2).

359 The I/(I+H) ratio within the various krill body fractions can reveal recent and past feeding history  
360 (Fig. 9A-D). Thus, the stomach, gut, faecal pellets and digestive gland showed similar I/(I+H) ratios  
361 within the same individual, indicative of their recent feeding history. In contrast, muscle and remaining  
362 body tissue often had different ratios as they integrate diet information over longer times. Highest  
363 I/(I+H) ratios in krill stomachs were found at 5 stations closest to the ice edge in the western and central  
364 Scotia Sea, suggesting that krill were feeding on a diet enriched in sea ice diatoms. At 4 stations near  
365 the ice edge and up to ~200 km further north, krill had moderate I/(I+H) ratios in their stomachs  
366 indicating a mixed diet of ice-derived diatoms and open water diatoms. Low I/(I+H) ratios in krill  
367 stomachs, but higher ratios in their muscle and rest of the body were found at 11 stations ~200-600 km  
368 north of the ice edge, suggesting that krill had been feeding on ice diatoms in the past, but had switched  
369 to open water diatoms by the time of sampling. At 26 mainly northern stations, krill did not contain any  
370 detectable IPSO<sub>25</sub> and may, therefore, not have fed on ice diatoms at all.

371 The overall concentration of IPSO<sub>25</sub> and HBI III in krill and their I/(I+H) ratios showed some  
372 variability with body size. Small krill ( $\leq 0.1$  g dry mass) contained lower concentrations of IPSO<sub>25</sub> and



373 HBI III in their stomachs than larger krill ( $> 0.1$  g dry mass) (mean: 806 vs 9822 ng g<sup>-1</sup>,  $t$ -Test: -3.14, df  
374 = 23,  $p = 0.005$ ). In their muscles, these differences were less pronounced (mean: 74.8 vs 195 ng g<sup>-1</sup>,  $t$ -  
375 Test: -2.63, df = 34,  $p = 0.013$ ). However, the  $I/(I+H)$  ratios in krill stomachs did not show any  
376 relationship with body mass (Fig. 9E). High  $I/(I+H)$  ratios were found in both small and large krill,  
377 indicating equal access to sea ice diatoms. Likewise, medium and low  $I/(I+H)$  ratios occurred across the  
378 sampled size range of krill suggesting that they switched simultaneously from feeding on sympagic to  
379 pelagic diatoms. In krill muscle, maximum  $I/(I+H)$  ratios were lower than in the stomach and ratios  
380 showed a linear drop with body size (Fig. 9F). A likely explanation is that krill had been feeding on sea  
381 ice diatoms for a relatively short time only. During this time,  $I/(I+H)$  ratios in their muscle did not  
382 equilibrate with values in their diet. This applies to small krill with fast turnover rates and even more so  
383 to large krill with longer integration times.

384

### 385 *3.5 Krill performance under different feeding conditions*

386 Based on our analysis, three groups of krill can be distinguished: those that had been feeding on  
387 ice diatoms (high IP<sub>SO<sub>25</sub></sub> content), those that had been feeding on open-water diatoms favoured by  
388 conditions at the receding ice edge (high HBI III content) and those that did not feed substantially on  
389 either of these diatoms (no/ low IP<sub>SO<sub>25</sub></sub> or HBI III content). To establish whether one of these feeding  
390 histories gave krill an advantage in their condition and performance, we tested three indicators: their  
391 mass-length-ratio, the size of their digestive gland and their growth rate. However, as each of these  
392 indicators correlates with krill body size, we present the residuals of the indicator-to-body size  
393 regression rather than absolute values (i.e. size of digestive gland-to-total mass regressions, growth rate-  
394 to-length regression and mass-to-length regression). Using this approach, we found that krill were in  
395 best condition near the ice edge in the eastern Scotia Sea (Stn 47) with positive residuals for all three  
396 indicators (Fig. 10A-C). Krill sampled at the ice edge in the central Scotia Sea (Stn 20, 31) and at South  
397 Georgia (Stn 56-61) showed positive residuals for at least two of these parameters. Overall, the  
398 residuals of the krill mass-length regression were mostly positive in the central and eastern Scotia Sea  
399 and at South Georgia, but negative in the western Scotia Sea. This is likely due to local differences in  
400 the food availability, as indicated by the significant positive relationship between mass-residual and *in*  
401 *situ* chl *a* concentration (Fig. 10D). On average, a high IP<sub>SO<sub>25</sub></sub> content in krill was associated with low  
402 chl *a* concentrations and therefore ‘below average’ krill body mass, while a high HBI III content in krill  
403 co-occurred with medium chl *a* concentrations and more often with ‘above average’ body mass (Fig.  
404 10D).



### 405 3.6 Recruitment of large calanoid copepods

406 Another important group of pelagic grazers in the Southern Ocean are calanoid copepods, e.g. the  
407 high-latitude species *Calanoides acutus* and *Calanus propinquus*. While HBIs have not been measured  
408 in these species, their overall abundance and age structure gives some information about suitable  
409 feeding grounds. For both species, abundances were highest at South Georgia and in the south-eastern  
410 Scotia Sea (Fig. 11A). The latter site was dominated by young development stages (copepodite stages I-  
411 III), which indicates recent successful recruitment (Fig. 11B). At South Georgia, the population was  
412 older, but also dominated by new recruits (copepodite stage IV). In contrast, in the western Scotia Sea  
413 copepod abundances were low, overall, and the population consisted of ‘overwintered’ copepodite stage  
414 V and females, suggesting that recruitment was delayed or had failed.

415

## 416 4. Discussion

### 417 4.1 Evaluating the HBI approach

418 Knowledge about the role of ice algae- vs. phytoplankton-produced carbon for higher trophic levels  
419 is central to our understanding of polar ecosystems. However, reliable estimates are difficult to achieve.  
420 Firstly, traditional trophic markers such as fatty acids, accessory pigments or taxonomy are of limited  
421 use as diatoms often dominate both communities with few species being obligate ice inhabitants  
422 (Garrison et al. 1987, Lizotte 2001, Arrigo 2017). Secondly, approaches that allow the separation of the  
423 two sources based on non-conservative tracers, including bulk- or compound-specific stable isotope  
424 analysis, rely on numerous assumptions that are not always met in practice (Budge et al. 2008). An  
425 example is isotopic fractionation, where the  $\delta^{13}\text{C}$  values of fatty acids derived from diatoms, and not  
426 produced *de novo* by the consumer [e.g. 16:4(n-1) or 20:5(n-3)] are usually assumed to remain  
427 unchanged across trophic levels (e.g. Budge et al. 2008, Wang et al. 2015, Kohlbach et al. 2017).  
428 However, laboratory and field studies have shown significant isotopic fractionation (-4 to -1‰) in  
429 polyunsaturated fatty acids between diet and consumer, and a gradual depletion in the  $^{13}\text{C}$  content of  
430 fatty acids upward through the food chain (Bec et al. 2011, Gladyshev et al. 2012 and ref. therein). If  
431 this isotopic fractionation remains unaccounted for, the contribution of the isotopically lighter source is  
432 overestimated and this bias increases with shorter isotopic distance between the endmembers (Bec et al.  
433 2011). Based on data obtained from Antarctic krill by Kohlbach et al. (2017), the ice algae source of  
434 20:5(n-3) increased from 64 to 89% in larvae, from 46 to 70% in juveniles and from -18 to 7% in adults  
435 if a fractionation of -1.5‰ between diatoms and grazer was implemented, according to Bec et al.



436 (2011). This illustrates that the interpretation of fatty acid-specific stable isotope data can be severely  
437 skewed if possible 'digestive'  $^{13}\text{C}$  depletion of fatty acids is not considered (Gladyshev et al. 2012).

438 In contrast to fatty acids, where one marker [e.g. 20:5(n-3)] carries the mixed isotopic signal from  
439 two food sources with additional fractionation within the grazer, the HBI approach is more straight-  
440 forward. Here, two independent markers exist, one for ice algae (IPSO<sub>25</sub>) and one for phytoplankton  
441 (HBI III). Thus, if IPSO<sub>25</sub> occurred in krill in the present study, it unambiguously indicated their  
442 consumption of ice algae. Moreover, the relative abundance of IPSO<sub>25</sub> and HBI III [I/(I+H)] remained  
443 the same during transfer from krill stomach to the digestive gland (Fig. 9), which suggests that there  
444 was no selective absorption or degradation within the grazer. This is in line with laboratory experiments  
445 which showed near identical HBI ratios in the brine shrimp *Artemia* sp. and its food (Brown and Belt  
446 2017). Thus, key advantages of the HBI approach are the existence of a sea ice proxy and its open water  
447 counterpart, and minimal signature alterations by the consumer.

448 On the other hand, disadvantages of the HBI approach may arise from the generally lower abundance  
449 of these markers. While fatty acids are ubiquitous to marine life, HBIs are only produced by certain  
450 diatom species (Brown et al. 2014, Belt et al. 2017 and references therein). Four such species are  
451 currently known to produce the Arctic sea ice proxy IP<sub>25</sub> (Brown et al. 2014), while in the Southern  
452 Ocean so far only one diatom species has been identified as a source of IPSO<sub>25</sub> (viz. *Berkeleya*  
453 *adeliensis*, Belt et al. 2016). The four Arctic source species are considered omnipresent in sea ice,  
454 however, and the application of IP<sub>25</sub> as a proxy for palaeo Arctic sea ice reconstructions is well  
455 established (Belt and Müller 2013). In contrast, research effort on HBIs in the Southern Ocean started  
456 more recently and initial findings require further confirmation. For instance, the known Antarctic source  
457 of IPSO<sub>25</sub>, *B. adeliensis*, is commonly associated with landfast ice and blooms in spring/ early summer,  
458 which may limit its use as a sea ice proxy in oceanic settings or during winter (Belt et al. 2016).  
459 However, sediment cores, sea ice samples, water samples and Antarctic predators indicate a widespread  
460 occurrence of IPSO<sub>25</sub>, including coastal- and open ocean regions, and samples obtained in summer and  
461 winter (this study, Massé et al. 2011, Goutte et al. 2013, Collins et al. 2013). This suggests co-  
462 production of IPSO<sub>25</sub> by as yet unidentified source species or by *B. adeliensis* inhabiting also non-  
463 coastal sea ice.

464 The proportion of IPSO<sub>25</sub> in the combined IPSO<sub>25</sub> and HBI III pool [I/(I+H) as presented in this  
465 study] is only a relative indicator of ice algae- vs. phytoplankton produced carbon. A translation into  
466 carbon values would require that the POC-to-HBI ratio is estimated for the local end-members (ice



467 algae, phytoplankton) and that I/(I+H) ratios are calibrated with known proportions of these end-  
468 members. Such calibration has been carried out for ratios of pelagic- vs. sympagic HBIs common in the  
469 Arctic via the so-called HBI-fingerprint ('H-print'; Brown and Belt 2017), and subsequently applied to  
470 obtain quantitative estimates of ice-derived carbon in Arctic amphipods (Brown et al. 2017). However,  
471 in this study we did not assess the absolute amount of carbon that krill acquire from ice algae. Instead  
472 we aimed for a mechanistic understanding of the role of sea ice for grazers such as krill, considering  
473 both carbon-production within sea ice and conditioning effects of sea ice that promote phytoplankton  
474 blooms.

475 After the initial application of HBIs as trophic markers in Southern Ocean food web studies by  
476 Goutte et al. (2013, 2014a, 2014b), our results provide three lines of evidence for the robustness of this  
477 approach: First, the carbon isotopic signatures ( $\delta^{13}\text{C}$ ) of IPSO<sub>25</sub> and HBI III confirm their different  
478 origins in sympagic vs. pelagic diatoms (Table 1). Second, given our open water set of sampling  
479 stations, both HBIs occurred in highest concentrations in suspended matter near the retreating ice edge;  
480 but they were associated with different oceanographic conditions. IPSO<sub>25</sub> coincided with sea ice cover  
481 and low temperatures, while HBI III peaked where melt water-driven stratification and enhanced chl *a*  
482 concentrations indicate favourable conditions for phytoplankton growth (Fig. 6). Third, there was a  
483 spatial overlap in the occurrence of HBIs in suspended matter and krill, which points to a direct trophic  
484 transfer (Fig. 5). The I/(I+H) ratios in krill stomachs, and therefore the dietary role of ice diatoms,  
485 decreased with the stations distance from the ice edge (Fig. 9). In conclusion, the HBI approach has  
486 delivered plausible results and overcomes some of the limitations of other trophic markers. Therefore,  
487 we consider it a suitable tool to assess the role of ice algae and ice-conditioned phytoplankton for  
488 Southern Ocean grazers. However, given the different strengths and weaknesses of HBI, fatty acid-  
489 specific stable isotopes and other trophic markers, their combined application is likely to increase the  
490 robustness of the results and the amount of detail revealed (Schmidt et al. 2006).

491

#### 492 *4.2 The role of ice algae-produced carbon for krill nutrition*

493 Krill feeding on ice algae is usually envisaged as larval krill accumulating under sea ice in search for  
494 winter food (Daly 2004), or juvenile and adult krill scraping off algae from the ice underside during the  
495 spring bloom (Marschall 1988) resulting in intensive downward flux of krill faecal pellets (Michels et  
496 al. 2008). However, here the ice proxy IPSO<sub>25</sub> revealed that ice algae can be an important food source  
497 for krill in early summer, even several weeks after the ice cover has disappeared. These considerations  
498 are based on the occurrence of IPSO<sub>25</sub> in the krill stomach, which contains food ingested within a



499 couple of hours before capture (Schmidt and Atkinson 2016), and therefore relates to the environment at  
500 the sampling location. At five stations near the ice edge, krill stomachs contained a higher proportion of  
501 ice algae [ $I/(I+H)_{\text{Stomach}}$ :  $0.93 \pm 0.03$ ] than the suspended matter in surface waters [ $I/(I+H)_{\text{SM}}$ :  $0.68 \pm 0.21$ ].  
502 Up to 200 km north of the current ice edge, krill still ingested a mixture of ice algae and phytoplankton  
503 [ $I/(I+H)_{\text{Stomach}}$ :  $0.56 \pm 0.24$ ], while  $\text{IPSO}_{25}$  was not detected in suspended matter from surface waters.  
504 These observations suggests that krill fed preferentially on ice algae and sampled them below the upper  
505 mixed layer, either during their diurnal vertical migration or in special foraging trips towards the  
506 benthos (Clarke and Tyler 2008, Schmidt et al. 2011). At Stn 8, for instance, a high  $I/(I+H)$  ratio  
507 coincided with lithogenic particles in krill stomachs, which may have been ingested at the seabed  
508 (Schmidt et al. 2011). About 200-600 km north of the ice edge,  $\text{IPSO}_{25}$  was found in krill muscle tissue,  
509 but not in their stomachs. Lipids in krill muscle tissue have a much slower turnover rate than those in  
510 the stomach and can therefore give information about the feeding history within the last few weeks.  
511 Here, the results indicate that krill had been feeding on ice algae in the past, but subsequently relied on  
512 phytoplankton. Overall,  $\text{IPSO}_{25}$  was detected in krill from 21 stations across the western and central  
513 Scotia Sea, confirming the widespread uptake of ice algae as a food source.

514 Krill stomach and muscle showed different trends between body mass and the  $I/(I+H)$  ratio,  
515 suggesting that krill had only been feeding on ice algae for a relatively short period. Small krill were  
516 equilibrated with the ice algae diet, having high  $I/(I+H)$  ratios in both stomach and muscle, while larger  
517 krill had high  $I/(I+H)$  ratios only in their stomachs and not in their muscles (Fig. 9). This suggests that  
518 larger krill did not feed long enough on ice algae to reach equilibrium between diet and body tissue.  
519 Most likely, ice algae became more accessible to krill when the ice started to melt (Jia et al. 2016). The  
520  $\text{IPSO}_{25}$  extracted from krill was enriched in  $\delta^{13}\text{C}$  (Table 1), as is typical for material from interior sea ice  
521 (McMinn et al. 1999, Wang et al. 2014) that is only within reach of krill when the algae are released  
522 into the water column. A carbon budget of ice algae in the Canadian Arctic in spring showed that >65%  
523 of the biomass, released from sea ice into the upper water column, remained suspended (Michel et al.  
524 1996). However, the high variability in chl *a* residence time (mean:  $31 \pm 33$  days) and -sinking rate  
525 (mean:  $1.4 \pm 1.5 \text{ m d}^{-1}$ ) illustrates the dual fate of ice algae; while some rapidly sink out of the euphotic  
526 zone and efficiently transfers carbon to the benthos (e.g. Riebesell et al. 1991, Renaud et al. 2007,  
527 Amiraux et al. 2017), others remain suspended over several weeks and can aid the nutrition of pelagic  
528 grazers (Michel et al. 1996, Smik et al. 2016). In any case, the trophic importance of ice algae extends  
529 beyond the period of maximum production in sea ice (Michel et al. 1996).



530 In the western and central Scotia Sea, phytoplankton concentrations were low and the community  
531 was dominated by small size classes ( $< 12 \mu\text{m}$ ) during spring and summer 2002/2003 (Fig. 4, Korb et  
532 al. 2005). This may explain why krill continued feeding on ice algae even after they had descended out  
533 of surface waters. In some years, phytoplankton blooms seem not to take off in this region, and light  
534 limitation, iron deficiency and grazing pressure have been discussed as potential reasons (Lancelot et al.  
535 1993, Korb et al. 2005, Park et al. 2010). Our study period coincided with a negative phase of the  
536 Southern Annular Mode ([www.nerc-bas.ac.uk/public/icd/gjma/newsam.1957.2007.txt](http://www.nerc-bas.ac.uk/public/icd/gjma/newsam.1957.2007.txt)), which is  
537 characterised by reduced strength and duration of wind mixing events (Saba et al. 2014). This led to  
538 shallow mixed layers and deep euphotic depths, constituting favourable light conditions for  
539 phytoplankton growth (Fig. 4, Korb et al. 2005). However, 2002/2003 was also a year of good krill  
540 recruitment (Atkinson et al. 2014) and high krill densities occurred especially in the western and central  
541 Scotia Sea (authors' unpubl. observations). At 7 stations in the central Scotia Sea, krill contained high  
542 amounts of HBI III ( $110\text{--}3460 \text{ ng g}^{-1}$ , esp. Stn 22, Fig. 5), even though there was little evidence of HBI  
543 III in the suspended matter in surface waters at that time. This suggests that diatom species favoured  
544 within the MIZ were produced in the central Scotia Sea, but did not accumulate, possibly due to high  
545 grazing losses. A longer-term data set of satellite-derived chl *a* concentrations shows that the area where  
546 krill contained high amounts of HBI III (Fig. 5E) matches the region with exceptionally low surface chl  
547 *a* concentrations in the central Scotia Sea in the 2002/2003 season (Fig. 3E).

548 The combination of high krill densities and low food availability can lead to competition-induced  
549 starvation (Ryabov et al. 2017). Such an effect may be seen in the krill' weight-to-length ratios: At most  
550 stations in the western and central Scotia Sea, krill were lighter than predicted from their body length,  
551 showing negative residuals from the mass-length regression (Fig. 10c). These stations largely coincided  
552 with those where krill contained the ice proxy IPSO<sub>25</sub>. However, the presence of IPSO<sub>25</sub> in krill distant  
553 from the ice edge may simply indicate a shortage of their summer food – phytoplankton. More relevant  
554 is the link between IPSO<sub>25</sub> and krill performance at stations near the ice edge, where ice algae were  
555 prominent in their stomachs. Of these six stations, two provided good feeding conditions for krill  
556 (positive residuals, Stn 20, 31), while four did not (negative residuals, Stn 5, 6, 18, 30). This is in line  
557 with other studies showing high variability in food supply from sea ice (Marschall et al. 1988, Daly  
558 2004, Michels et al. 2008, Schmidt et al. 2012, 2014, Meyer et al. 2017). Local differences in snow  
559 cover, ice thickness, ice rafting or time of ice formation can lead to different concentrations of ice algae  
560 in the bottom ice layer (Fritsen et al. 2008, Meiners et al. 2012). However, below-average krill body  
561 mass was even found in individuals that contained high concentrations of IPSO<sub>25</sub> (Stn. 5, 18), while krill



562 with positive residuals from the mass-length regression showed high concentrations of both IPSO<sub>25</sub> and  
563 HBI III (Stn 30) or mainly HBI III (Stn 20). This indicates an essential role of phytoplankton for krill  
564 performance in spring, as has been suggested previously (Cuzin-Roudy et al. 1992, Schmidt et al.  
565 2012).

566

#### 567 *4.3 The role of ice-conditioned phytoplankton blooms*

568 Off-shore regions of the Southern Ocean are often characterised by high-nitrate-low-chlorophyll  
569 (HNLC) conditions due to the shortage of iron. However, in the Scotia Sea primary and secondary  
570 production can be comparatively high (Atkinson et al. 2004, Park et al. 2010). In 2002/2003, late sea ice  
571 retreat coincided with a negative phase of the Southern Annular Mode, volcanic activity at Mount  
572 Belinda (~ 80 km east off Stn. 50) and high krill abundances (authors' unpublished observations,  
573 Patrick et al. 2005, Ward et al. 2006). This would have provided favourable light conditions and iron  
574 (Korb et al. 2005, Browning et al. 2014, Schallenberg et al. 2015), but also enhanced grazing impact  
575 and nutrient recycling (Schmidt et al. 2016). Perhaps as a consequence, the phytoplankton bloom was  
576 unusually long-lasting and intensive across the East Scotia Ridge, but weaker than average in the central  
577 Scotia Sea (Fig. 3; Park et al. 2010). Sea ice retreat can assist phytoplankton growth due to the freshness  
578 of the meltwater, following brine rejection during its formation. The low-salinity input enhances water  
579 column stability, thereby reducing vertical mixing and retaining phytoplankton in an optimal light  
580 environment (Smith and Nelson 1986). However, meltwater lenses do not always lead to ice edge  
581 blooms. In the western and central Scotia Sea, strong density gradients occurred upon ice retreat but  
582 phytoplankton did not accumulate. In contrast, in the east, blooms propagated behind the receding ice  
583 edge over hundreds of kilometres and for several months (Fig. 3). A reason for these differences may be  
584 the speed of ice retreat (Constable et al. 2003). Between mid December and mid February, ice retreated  
585 at ~1.7 km d<sup>-1</sup> in the west and at 11.7 km d<sup>-1</sup> in the east (authors' unpublished data). Rapid ice retreat  
586 enhances the volume and spatial extent of meltwater input and therefore the likelihood that stratification  
587 persists long enough for marked phytoplankton growth and accumulation (Smith and Nelson 1986,  
588 Smith et al. 2006). Other factors controlling phytoplankton development along the receding ice-edge  
589 include iron deficiency and grazing pressure by zooplankton (Tréguer and Jacques 1992, Lancelot et al.  
590 1993).

591 Ice-edge phytoplankton blooms have been reported throughout the Arctic (Perrette et al. 2011) and  
592 from the Ross Sea, Weddell Sea, Scotia Sea, Prydz Bay and the Pacific sector of the Southern Ocean  
593 (e.g. Smith and Nelson 1986, Nelson et al. 1987, Sullivan et al. 1988, Comiso et al. 1993, Moore et al.



594 1999, Constable et al. 2003). However, the overall importance of primary production in the MIZ is still  
595 debated (Vancoppenolle et al. 2013). Originally, the MIZ was considered a major hotspot for  
596 autotrophic production in the Southern Ocean (Smith and Nelson 1986). Subsequent analysis of satellite  
597 data, however, suggests that phytoplankton blooms in the MIZ are largely suppressed at high wind  
598 speed, and even with lower winds, blooms occur only over one-third of the MIZ (Fitch and Moore  
599 2007). Therefore, area-normalised primary production rates calculated from ocean colour are on  
600 average only slightly higher in the MIZ than in the permanently ice-free Southern Ocean (Arrigo et al.  
601 2008). This has led to the conclusion that while the MIZ has the potential to be productive, physical  
602 conditions are seldom conducive to the development of intense, longer-lived phytoplankton blooms  
603 (Arrigo et al. 2008). On the other hand, high abundances of zooplankton, seabirds and whales are  
604 characteristic of the MIZ and confirm enhanced biological activity and the importance of this region for  
605 the food web (Brown and Lockyer 1984, Ichii et al. 1990, Ainley et al. 2017).

606 Antarctic krill sampled in the previously ice covered eastern Scotia Sea had high HBI III  
607 concentrations and above-average body mass (i.e. positive residuals in Fig. 10c). The occurrence of HBI  
608 III in krill tissue often coincided with medium to high chl *a* concentrations in the water column (Fig.  
609 10d). Therefore, enhanced krill performance in the east is most likely a result of higher food  
610 concentrations. A number of studies has previously found chl *a* concentrations to represent a reliable  
611 predictor of krill growth and maturation (Ross et al. 2000, Atkinson et al. 2006, Schmidt et al. 2012,  
612 Meyer et al. 2017). Krill from the most southerly station of the eastern transects (Stn 47) were in  
613 similarly good conditions to those at South Georgia, showing high body mass, large digestive gland and  
614 exceptionally high growth rates when adjusted for their length. This is unexpected considering that, at  
615 the time of sampling, only 2 weeks of elevated chl *a* concentrations ( $>0.5 \text{ mg m}^{-3}$ ) were recorded at Stn.  
616 47, but ~16 weeks at South Georgia (based on ocean colour data, Fig. 2). A previous study revealed that  
617 krill can engage in “superfluous” feeding when food is abundant (Schmidt et al. 2012). This way, the  
618 food concentration in their digestive tract remains high and nutrient absorption per unit time is  
619 maximised. Consequently, krill can rapidly improve their body condition and advance in maturation  
620 (Schmidt et al. 2012). IPSO<sub>25</sub> was not detected in krill from Stn. 47, but was found in low  
621 concentrations in suspended matter at the neighbouring station closer to the ice edge (Stn. 48). Station  
622 47 had been ice free for ~20 days when krill were sampled, which is approximately the turnover-time of  
623 the Arctic sea ice proxy in zooplankton (Brown and Belt 2012). Therefore, krill may have been feeding  
624 on ice algae at this station, but any indication of this via IPSO<sub>25</sub> was lost following their switch to  
625 phytoplankton.



626 A few copepod species inhabit Antarctic sea ice, but the biomass dominant copepod grazers in high  
627 latitudes, *Calanoides acutus* and *Calanus propinquus*, are only loosely associated with sea ice, if at all  
628 (Arndt and Swadling 2006). *C. acutus* shows reduced feeding activity within the ice and their offspring  
629 only occur in the MIZ or open waters (Atkinson and Shreeve 1995, Burghart et al 1999). In contrast, *C.*  
630 *propinquus* have been found feeding on ice algae and spawning below sea ice, but their populations  
631 likewise expand mainly in open waters (Atkinson and Shreeve 1995, Burghart et al 1999). Both species  
632 can complete their life cycle at South Georgia (Atkinson et al. 1988), which is permanently sea ice-free.  
633 During our study period, the occurrence and recruitment of these species showed similarities to feeding  
634 behaviour and performance of Antarctic krill. In the western and central Scotia Sea, *C. acutus* and *C.*  
635 *propinquus* had low abundances and the populations were dominated by females and late copepodite  
636 stages representing the ‘old, overwintered’ generation. This delay or failure of recruitment was likely  
637 caused by the lack of phytoplankton, as also indicated by krill feeding on sinking ice algae in open  
638 waters, and their below-average body mass. Highest copepod abundances in the south-east coincided  
639 with the dominance of early copepodite stages (i.e. the ‘new’ generation). This region of intensive  
640 copepod reproduction (Stn 45, 50, 51, 52) matches high HBI III concentrations in suspended matter and  
641 enhanced krill performance in the wake of retreating sea ice. We therefore suggest that the MIZ is an  
642 important nursery ground for these large copepod species, in line with previous findings (Atkinson and  
643 Shreeve 1995, Burghart et al. 1999). At South Georgia, the copepod populations of *C. acutus* and *C.*  
644 *propinquus* were further advanced in their seasonal development (dominated by medium copepodite  
645 stages of the ‘new’ generation), but the overall abundances were similar to those in the south.

646 The weak, sporadic link between large calanoid copepods and ice algae in the Antarctic contrasts  
647 with conditions in the Arctic. Here ice algae serve as an important food source for spawning females of  
648 *Calanus glacialis* (Søreide et al. 2010, Durbin and Casas 2013) and the early developmental stages of *C.*  
649 *hyperboreus* (Conover 1988). Average primary production rates in sea ice are considered lower in the  
650 Southern Ocean than in the Arctic (Arrigo 2017). In the Antarctic, ~85% of sea ice is annual and needs  
651 to be newly inhabited every year (Stammerjohn and Maksym 2017). However, as much of this sea ice  
652 forms over deep ocean, re-colonisation from the benthos or via lateral dispersion from perennial sea ice  
653 is unlikely, leaving the water column as the sole source (Arndt and Swadling 2006). In contrast, Arctic  
654 sea ice covers comparatively shallow waters, and traditionally has a larger proportion of perennial sea  
655 ice, which increases the chances of re-colonisation. Another factor influencing productivity in sea ice is  
656 the level of irradiance available to primary producers (Meiners et al. 2012). Antarctic pack ice  
657 experiences some of the largest snowfall rates on Earth, while melt ponds are widespread in the Arctic



658 (Vancoppenolle et al. 2013). The former attenuates light, whereas the latter efficiently transmits it to the  
659 underlying ocean.

660

## 661 **5. Conclusion**

662 Large parts of the Southern Ocean are characterised by low phytoplankton concentrations due to  
663 the lack of iron, strong vertical mixing or grazing and other losses. Our study suggests that in such  
664 areas, pelagic grazers may benefit from seasonal sea ice in two ways. Firstly, suspended or sinking ice  
665 algae can supplement their diet in spring and summer. Second, retreating sea ice enhances the likelihood  
666 of bloom formation due to shoaling of the mixed layer, supply of iron and/or release of a seeding  
667 population. Phytoplankton blooms initiated in the MIZ allow zooplankton to grow rapidly, gain body  
668 reserves and advance in their development. Therefore, current and future changes in sea ice will not  
669 only affect sympagic fauna, but also zooplankton species that inhabit open waters adjacent to it. The  
670 analysis of two source-specific highly branched isoprenoids provided a useful tool to trace ice-produced  
671 and ice-conditioned food sources within pelagic grazers. Essential for their further application will be to  
672 resolve the spatial and temporal occurrence of the ice proxy IPSO<sub>25</sub>, and to gauge the carbon-to-  
673 isoprenoid ratios of ice algae and phytoplankton. Development of the HBI trophic marker approach,  
674 alongside other methods, will help us to understand exactly how Arctic and Antarctic food webs depend  
675 on sea ice.

676

## 677 **ACKNOWLEDGMENTS**

678 We thank the officers, crew, and scientists onboard the RRS *James Clark Ross* for their professional  
679 support during JR82. We acknowledge the MODIS mission scientists and associated NASA personnel  
680 for the production of data in the Giovanni online data system. We thank R. Korb for providing size-  
681 fractionated chl *a* measurements, and P. Cabedo-Sanz and L. Smik for help with lab work. This study  
682 was supported by a Research Project Grant (RPG-2014-021) awarded by the Leverhulme Trust (UK).  
683 A.A. was part-funded by NERC and Department for Environment, Food and Rural Affairs (DEFRA)  
684 grant NE/L 003279/1 (Marine Ecosystems Research Program).

685

## 686 **REFERENCES**

687 Ainley, D., Woehler, E.J., and Lescroël, A.: Birds and Antarctic sea ice, In: 'Sea Ice', ed. D. N. Thomas  
688 (Chichester: John Wiley & Sons, Ltd), 570–582, doi:10.1002/9781118778371.ch24, 2017.



- 689 Amiraux, R., Belt, S.T., Vaultiera, F., Galindoc, V., Gosselin, M., Bonina, P., Rontani, J.-F.:
- 690 Monitoring photo-oxidative and salinity-induced bacterial stress in the Canadian Arctic using
- 691 specific lipid tracers. *Mar. Chem.*, 194, 89-99, doi: 10.1016/j.marchem.2017.05.006, 2017.
- 692 Armand, L., Ferry, A., and Leventer, A.: Advances in palaeo sea ice estimation, In: 'Sea Ice', ed. D. N.
- 693 Thomas (Chichester: John Wiley & Sons, Ltd), 600–629, doi: 10.1002/9781118778371.ch26, 2017.
- 694 Arndt, C.E., and Swadling, K.M.: Crustacea in Arctic and Antarctic sea ice: distribution, diet and life
- 695 history strategies, *Adv. Mar. Biol.*, 51, 197-315, doi: 10.1016/S0065-2881(06)51004-1, 2006.
- 696 Arrigo, K.: Sea ice as a habitat for primary producers, In: 'Sea Ice', ed. D. N. Thomas (Chichester: John
- 697 Wiley & Sons, Ltd), 352–369, doi: 10.1002/9781118778371.ch14, 2017.
- 698 Arrigo, K. and Thomas, D.: Large scale importance of sea ice biology in the Southern Ocean, *Ant. Sc.*,
- 699 16, 471-486, doi: 10.1017/S0954102004002263, 2004.
- 700 Arrigo, K.R., van Dijken, L.G.L., and Bushinsky, S.: Primary production in the Southern Ocean, 1997-
- 701 2006, *J. Geophys. Res.*, 113, C08004, doi:10.1029/2007JC004551, 2008.
- 702 Atkinson, A. and Peck, J.M.: A summer-winter comparison of zooplankton in the oceanic area around
- 703 South Georgia. *Polar Biol.*, 8, 463-473, doi: 10.1007/BF00264723, 1988.
- 704 Atkinson, A. and Shreeve, R.S.: Response of the copepod community to a spring bloom in the
- 705 Bellingshausen Sea, *Deep-Sea Res. II*, 42, 1291-1311, doi: 10.1016/0967-0645(95)00057-W, 1995.
- 706
- 707 Atkinson, A., Siegel, V., Pakhomov, E., and Rothery P.: Long-term decline in krill stock and increase in
- 708 salps within the Southern Ocean, *Nature*, 432, 100-103, doi:10.1038/nature02996, 2004.
- 709 Atkinson, A., Shreeve, R., Hirst, A.G., Rothery, P., Tarling, G., Pond, D., Korb, R.E., Murphy, E.J., and
- 710 Watkins, J.L.: Natural growth rates in Antarctic krill (*Euphausia superba*): II. Predictive models
- 711 based on food, temperature, body length, sex, and maturity stage, *Limnol. Oceanogr.*, 51, 973-987,
- 712 doi: 10.4319/lo.2006.51.2.0973, 2006.
- 713 Atkinson, A., Siegel, V., Pakhomov, E.A., Rothery, P., Loeb, V., Ross, R.M., Quetin, L.B., Schmidt,
- 714 K., Fretwell, P., Murphy, E.J., Tarling, G.A., and Fleming, A.H.: Oceanic circumpolar habitats of
- 715 Antarctic krill, *Mar. Ecol. Prog. Ser.*, 362, 1-32, doi: 10.3354/meps07498, 2008.
- 716 Atkinson, A., Hill, S.L., Barange, M., Pakhomov, E.A., Raubenheimer, D., Schmidt, K., Simpson, S.J.,
- 717 and Reiss, C.: Sardine cycles, krill declines, and locust plagues: Revisiting 'wasp-waist' food webs,
- 718 *Trends Ecol Evol.*, 29, 309-316, doi: 10.1016/j.tree.2014.03.011, 2014.
- 719 Barnes, D.K.A. and Tarling, G.A.: Polar oceans in a changing climate, *Current Biol.*, 27, 454-460, doi:
- 720 10.1016/j.cub.2017.01.045, 2017.



- 721 Bec, A., Perga, M-E., Koussoroplis, A., Bardoux, G., Desvillettes, C., Bourdier, G., and Mariotti, A.:
- 722 Assessing the reliability of fatty acid-specific stable isotope analysis for trophic studies. *Meth. Ecol.*
- 723 *Evolut.*, 2, 651-659, doi: 10.1111/j.2041-210X.2011.00111.x, 2011.
- 724 Belt, S.T., and Müller, J.: The Arctic sea ice biomarker IP<sub>25</sub>: a review of current understanding,
- 725 recommendations for future research and applications in Palaeo sea ice reconstructions. *Quat. Sci.*
- 726 *Rev.*, 79, 9-25, doi: 10.1016/j.quascirev.2012.12.001, 2013.
- 727 Belt, S.T., Brown, T.A., Navarro-Rodriguez, A., Cabedo-Sanz, P., Tonkin, A., and Ingle, R.: A
- 728 reproducible method for the extraction, identification and quantification of the Arctic sea ice proxy
- 729 IP<sub>25</sub> from marine sediments. *Analyt. Meth.*, 4, 705-713, doi: , 2012.
- 730 Belt, S.T., Cabedo-Sanz, P., Smik, L., Navarro-Rodriguez, A., Berben, S.M. P., Knies, J., and
- 731 Husum, K.: Identification of paleo Arctic winter sea ice limits and the marginal ice zone: optimised
- 732 biomarker-based reconstructions of the late Quaternary Arctic sea ice. *Earth Planet. Sci. Lett.*, 431,
- 733 127-139, doi:10.1016/j.epsl.2015.09.020, 2015.
- 734 Belt, S.T., Smik, L., Brown, T.A., Kim, J.-H., Rowland, S.J., Allen, C.S., Gal, J.-K., Shin, K.-H., Lee,
- 735 J.I., and Taylor, K.W.R.: Source identification and distribution reveals the potential of the
- 736 geochemical Antarctic sea ice proxy IPSO<sub>25</sub>. *Nat. Comms.*, 7, 12655, doi:10.1038/ncomms12655,
- 737 2016.
- 738 Belt, S.T., Brown, T.A., Smik, L., Tatrek, A., Wiktor, J., Stowasser, G., Assmy, P., Allen, C.S., and
- 739 Husum, K.: Identification of C<sub>25</sub> highly branched isoprenoid (HBI) alkenes in diatoms of the genus
- 740 *Rhizosolenia* in polar and sub-polar marine phytoplankton, *Org. Geochem.* 110, 65-72, doi:
- 741 10.1016/j.orggeochem.2017.05.007, 2017.
- 742 Bester, M.N., Bornemann, H., and McIntyre, T.: Antarctic marine mammals and sea ice. In: ‘Sea Ice’,
- 743 ed. D. N. Thomas (Chichester: John Wiley & Sons, Ltd), 534-555,
- 744 doi: 10.1002/9781118778371.ch22, 2017.
- 745 Bluhm, B., Swadling, K.M., and Gradinger, R.: Sea ice as habitat for macrograzers, In: ‘Sea Ice’, ed. D.
- 746 N. Thomas (Chichester: John Wiley & Sons, Ltd), 394–414, doi: 10.1002/9781118778371.ch16,
- 747 2017.
- 748 Brierley, A.S., Fernandes, P.G., Brandon, M.A., Armstrong, F., Millard, N.W., McPhail, S.D.,
- 749 Stevenson, P., Pebody, M., Perrett, J., Squires, M., Bone, D.G., and Griffiths, G.: Antarctic krill
- 750 under sea ice: Elevated abundance in a narrow band just south of the ice edge, *Science*, 295, 1890-
- 751 1892, doi:10.1126/science.1068574, 2002.
- 752 Brown, S.G. and Lockyer, C.H.: Whales. In: Laws, R.M. (ed) *Antarctic Ecology*, Vol 2.
- 753 Academic Press, London, p 717-781, 1984.



- 754 Brown, T.A. and Belt, S.: Closely linked sea ice-pelagic coupling in the Amundsen Gulf revealed by the  
755 sea ice diatom biomarker IP<sub>25</sub>, *J. Plankton Res.*, 34, 647-654, doi:10.1093/plankt/fbs045, 2012.
- 756 Brown, T.A. and Belt, S.: Biomarker-based H-Print quantifies the composition of mixed sympagic and  
757 pelagic algae consumed by *Artemia* sp., *J. Exp. Mar. Biol. Ecol.*, 488, 32-37, doi:  
758 10.1016/j.jembe.2016.12.007, 2017.
- 759 Brown, T.A., Belt, S., Tatarek, A. and Mundy, C.J.: Source identification of the Arctic sea ice proxy  
760 IP<sub>25</sub>. *Nat. Commun.*, 5, 4197, doi:10.1038/ncomms5197, 2014.
- 761 Brown, T.A., Assmy, P., Hop, H., Wold, A., and Belt, S.T.: Transfer of ice algae carbon to ice-  
762 associated amphipods in the high-Arctic pack ice environment. *J. Plankton Res.*, 39, 664-674,  
763 doi:10.1093/plankt/fbx030, 2017.
- 764 Browning, T.J., Bouman, H.A., Henderson, G.M., Mather, T.A., Pyle, D.M., Schlosser, C., Woodward,  
765 E.M.S., and Moore, C.M.: Strong responses of Southern Ocean phytoplankton communities to  
766 volcanic ash, *Geophys. Res. Lett.*, 41, 2851-2857, doi: 10.1002/2014GL059364, 2014.
- 767 Budge, S.M., Wooller, M.J., Springer, A.M., Iverson, S.J., McRoy, C.P., and Divoky, G.J.: Tracing  
768 carbon flow in an arctic marine food web using fatty acid-stable isotope analysis, *Oecologia*, 157,  
769 117-129, doi: 10.1007/s00442-008-1053-7, 2008.
- 770 Burghart, S.E., Hopkins, T.L., Vargo, G.A., and Torres, J.J.: Effects of rapidly receding ice edge on the  
771 abundance, age structure and feeding of three dominant calanoid copepods in the Weddell Sea,  
772 Antarctica, *Polar Biol.*, 22, 279-288, doi: 10.1007/S003000050421, 1999.
- 773 Caron, D.A., Gast, R.J., and Garneau, M.-E.: Sea ice as habitat for micrograzers, In: 'Sea Ice', ed D. N.  
774 Thomas (Chichester: John Wiley & Sons, Ltd), 370-393, doi: 10.1002/9781118778371.ch15, 2017.
- 775 Cavalieri, D. J., Parkinson, C.L., P. Gloersen, P., and Zwally, H.J.: Sea Ice Concentrations from  
776 Nimbus-7 SMMR and DMSP SSM/I-SSMIS Passive Microwave Data, Version 1. [Indicate subset  
777 used]. Boulder, Colorado USA. NASA National Snow and Ice Data Center Distributed Active  
778 Archive Center. doi: 10.5067/8GQ8LZQVL0VL. 1996 (updated: 2014).
- 779 Clarke, A. and Tyler, P.A.: Adult Antarctic krill feeding at abyssal depths, *Current Biol.*, 18 282-285,  
780 doi:10.106/j.cub.2008.01.059, 2008.
- 781 Collins, L.G., Allen, C.S., Pike, J., Hodgson, D.A., Weckström, K., and Massé, M.: Evaluating highly  
782 branched isoprenoid (HBI) biomarkers as a novel Antarctic sea-ice proxy in deep ocean glacial age  
783 sediments, *Quat. Sci. Rev.*, 79 87-98, doi:10.1016/j.quascirev.2013.02.004, 2013.
- 784 Comiso, J.C., McClain, C.R., Sullivan, C.W., Ryan, J.P., and Leonhard, C.L.: Coastal zone color  
785 scanner pigment concentrations in the Southern Ocean and relationships to geophysical surface  
786 features, *J. Geophys. Res.*, 98, 2419-2451, doi: 10.1029/92JC02505, 1993.



- 877 Conover, R.J.: Comparative life histories in the genera *Calanus* and *Neocalanus* in high latitudes of the  
878 Northern Hemisphere. *Hydrobiologia*, 167, 127-142, doi:10.1007/BF00026299, 1988.
- 879 Constable, A.J., Nicol, S., and Strutton, P.G.: Southern Ocean productivity in relation to spatial and  
880 temporal variation in the physical environment. *J. Geophys. Res.*, 108, 1-10, doi:  
881 10.1029/2001JC001270, 2003.
- 882 Constable, A.J. et al.: Climate change and Southern Ocean ecosystems I: how changes in physical  
883 habitats directly affect marine biota. *Glob. Change Biol.*, 20, 3004-3025, doi:10.1111/gcb.12623,  
884 2014.
- 885 Cuzin-Roudy, J. and Labat, J.P.: Early summer distribution of Antarctic krill sexual development in the  
886 Scotia-Weddell region: A multivariate approach. *Polar Biol.*, 12, 65-74, 1992.
- 887 Daly, K.: Overwintering growth and development of larval *Euphausia superba*: an interannual  
888 comparison under varying environmental conditions west of the Antarctic Peninsula. *Deep-Sea*  
889 *Res. II*, 51, 2139-2168, doi:10.1016/j.dsr2.2004.07.010, 2004.
- 890 Ducklow, H.W., Baker, K., Martinson, D.G., Quetin, L.B., Ross, R.M., Smith, R.C., Stammerjohn, S.E.,  
891 Vernet, M., and Fraser, W.: Marine pelagic ecosystems: the West Antarctic Peninsula, *Philos. Trans.*  
892 *R. Soc. Lond. B. Biol. Sci.*, 362, 67-94, doi: 10.1098/rstb.2006.1955, 2007.
- 893 Durbin, E.G. and Casas, M.: Early reproduction by *Calanus glacialis* in the Northern Bering Sea: the  
894 role of ice algae as revealed by molecular analysis. *J. Plank. Res*, 36, 523-541,  
895 doi:10.1093/plankt/fbt121, 2013.
- 896 Etourneau, J., Collins, L.G., Willmott, V., Kim, J.-H., Barbara, L., Leventer, A., Schouten, S.,  
897 Sinninghe Damsté, J.S., Bianchini, A., Klien, V., Crosta, X., and Massé, G.: Holocene climate  
898 variations in the western Antarctic Peninsula: evidence for sea ice extent predominantly controlled  
899 by changes in insolation and ENSO variability, *Climate of the Past*, 9, 1431-1446, doi: 10.5194/cp-  
900 9-1431-2013, 2013.
- 901 Fitch, D.T. and Moore, J.K.: Wind speed influence on phytoplankton bloom dynamics in the Southern  
902 Ocean marginal ice zone, *J. Geophys. Res.*, 112, C08006, doi: 10.1029/2006JC004061, 2007.
- 903 Flores, H., van Franeker, J.A., Siegel, V., Haraldsson, M., Strass, V., Meester, E.H., Bathmann, U., and  
904 Wolff, W.J.: The association of Antarctic krill *Euphausia superba* with the under-ice habitat. *PLoS*  
905 *ONE*, 7, e31775, doi:10.1371/journal.pone.0031775, 2012a.
- 906 Flores, H. et al.: Impact of climate change on Antarctic krill. *Mar. Ecol. Prog. Ser.*, 458, 1-19, doi:  
907 10.3354/meps09831, 2012b.
- 908 Forcada, J. and Hoffman, J.I.: Climate change selects for heterozygosity in a declining fur seal  
909 population, *Nature*, 511, 462-465, doi:10.1038/nature13542. 2014.



- 820 Fraser, W. and Hoffmann, E.: A predator's perspective on causal links between climate change,  
821 physical forcing and ecosystem response, *Mar. Ecol. Prog. Ser.*, 265, 1-15, doi:  
822 10.3354/meps265001, 2003.
- 823 Fritsen, C.H., Memmott, J., and Stewart, F.J.: Inter-annual sea-ice dynamics and micro-algal biomass in  
824 winter pack ice of Marguerite Bay, Antarctica, *Deep-Sea Res. II*, 55, 2059-2067, doi:  
825 10.1016/j.dsr2.2008.04.034, 2008.
- 826 Garrison, D.L., Buck, K.R., and Fryxell, G.A.: Algal assemblages in Antarctic pack-ice and in ice-edge  
827 plankton, *J. Phycol.*, 23, 564-572, doi: 10.1111/j.1529-8817.1987.tb04206.x, 1987.
- 828 Gladyshev, M.I., Sushchik, N.N., Kalachova, G.S. and Makhutova, O.N.: Stable isotope composition of  
829 fatty acids in organisms of different trophic levels in the Yenisei River, *PloS ONE*, 7, e34059, doi:  
830 10.1371/journal.pone.0034059, 2012.
- 831 Goutte, A., Cherel, Y., Houssais, M-N., Klein, V., Ozouf-Costaz, C., Raccut, M., Robineau, C., and  
832 Massé, G.: Diatom-specific highly branched isoprenoids as biomarkers in Antarctic consumers,  
833 *PloS ONE*, 8, e56504, doi:10.1371/journal.pone.0056504, 2013.
- 834 Goutte, A., Charrassin, J-B., Cherel, Y., Carravieri, A, De Grissac, S., and Massé, G.: Importance of ice  
835 algal production for top predators: new insights using sea-ice biomarkers, *Mar. Ecol. Prog. Ser.*,  
836 513, 269-275, doi:10.3354/meps10971, 2014a.
- 837 Goutte, A., Cherel, Y., Ozouf-Costz, C., Robineau, C., Lanshere, J. and Massé, G.: Contribution of sea  
838 ice organic matter in the diet of Antarctic fishes: a diatom-specific highly branched isoprenoid  
839 approach. *Polar Biol.*, 37, 903-910, doi:10.1007/s00300-014-1489-7, 2014b
- 840 Grebmeier, J.M., Moore, S.E., Overland, J.E., Frey, K.E, and Gradinger, R.: Biological responses to  
841 recent Pacific Arctic sea ice retreat, *Trans. Am. Geophys. Union*, 91, 161-162, doi:  
842 10.1029/2010EO180001, 2010.
- 843 Hagen, W., and Auel, H.: Seasonal adaptations and the role of lipids in oceanic zooplankton, *Zoology*,  
844 104, 313-326, doi: 10.1078/0944-2006-00037, 2001.
- 845 Ichii, T.: Distribution of Antarctic krill concentrations exploited by Japanese krill trawlers and mink  
846 whales, *Proc. NIPR Symp. Polar Biol.*, 3, 36-56, 1990.
- 847 Jia, Z., Swadling, K.M., Meiners, K.M., Kawaguchi, S., and Virtue, P.: The zooplankton food web  
848 under East Antarctic pack ice – A stable isotope study, *Deep-Sea Res. II*, 131, 189-202, doi:  
849 10.1016/j.dsr2.2015.10.010, 2016.
- 850 Kawaguchi, S., Nicol, S., and Press, A.J.: Direct effects of climate change on the Antarctic krill fishery,  
851 *Fish. Manag. Ecol.*, 16, 424-427, doi: 10.1111/j.1365-2400.2009.00686.x, 2009.



- 852 Kohlbach, D., Lange, B.A., Schaafsma, F.L., David, C., Vortkamp, M., Graeve, M., van Franeker, J.A.,  
853 Krumpfen, T., and Flores, H.: Ice algae-produced carbon is critical for overwintering of Antarctic  
854 krill *Euphausia superba*. *Front. Mar. Sci.*, 4, 310, doi: 10.3389/fmars.2017.00310, 2017.
- 855 Korb, R.E., Whitehouse, M.J., Thorpe, S.E., and Gordon M.: Primary production across the Scotia Sea  
856 in relation to the physic-chemical environment, *J. Mar. Syst.*, 57, 231-249, doi:  
857 10.1016/j.jmarsys.2005.04.009, 2005.
- 858 Kottmeier, S.T. and Sullivan, C.W., Late winter primary production and bacterial production in sea ice  
859 and seawater west of the Antarctic Peninsula, *Mar. Ecol. Prog. Ser.*, 36, 287–298,  
860 doi:10.3354/meps036287,1987.
- 861 Lancelot, C., Mathot, S., Veth, C., and de Baar, H.: Factors controlling phytoplankton ice-edge blooms  
862 in the marginal ice-zone of the northwestern Weddell Sea during sea ice retreat 1988: field  
863 observations and mathematical modelling, *Polar Biol.*, 13, 377-387, 1993.
- 864 Lannuzel, D., Schoemann, V., de Jong, J., Pasquer, B., van der Merwe, P., and Bowie, A.R.:  
865 Distribution of dissolved iron in Antarctic sea ice: spatial, seasonal and inter-annual variability, *J.*  
866 *Geophys. Res.*, 115, G03022, doi:10.1029/2009JG001031, 2010.
- 867 Leu, E., Søreide, J.E., Hessen, D.O., Falk-Petersen, S., and Berge, J.: Consequences of changing sea-  
868 ice cover for primary and secondary producers in the European Arctic shelf seas: Timing, quantity,  
869 and quality, *Prog. Oceanogr.* 90, 18-32, doi: 10.1016/j.pocean.2011.02.004, 2011.
- 870 Li, W.K.W., McLaughlin, F.A., Lovejoy, C., and Carmack, E.C.: Smallest algae thrive as the Arctic  
871 Ocean freshens, *Science*, 326, 539, doi:10.1126/sciece.1179798, 2009.
- 872 Lizotte, M.P.: The contribution of sea ice algae to Antarctic marine primary production, *Am. Zoolog.*,  
873 41, 57-73, doi:10.1093/icb/41.1.57, 2001.
- 874 Marchese, C., Albouy, C., Tremblay, J-E., Dumont, D., D'Ortenzio, F., Vissault, S., and Bélanger, S.:  
875 Changes in phytoplankton bloom phenology over the North Water (NOW) polynya: a response to  
876 changing environmental conditions, *Polar Biol.*, doi: 10.1007/s00300-017-2095-2, 2017.
- 877 Marschall, P.: The overwintering strategy of Antarctic krill under the pack ice of the Weddell Sea, *Polar*  
878 *Biol.*, 34, 1887-1900, doi: 10.1007/BF00442041, 1988.
- 879 Massé, G., Belt, S.T., Crosta, X., Schmidt, S., Snape, I., Thomas, D.N., and Rowland, S.J.: Highly  
880 branched isoprenoids as proxies for variable sea ice conditions in the Southern Ocean. *Ant. Sci.*, 23,  
881 487-498, doi: 10.1017/S0954102011000381, 2011.
- 882 McMinn, A., Skerratt, J., Trull, T., Ashworth, C., and Lizotte, M.: Nutrient stress gradient in the bottom  
883 5 cm of fast ice, McMurdo Sound, Antarctica. *Polar. Biol.*, 21, 220-227,  
884 doi: 10.1007/s003000050356, 1999.



- 885 Meier, W.N.: Losing Arctic sea ice: observations of the recent decline and the long-term context. In:  
886 ‘Sea Ice’, ed. D. N. Thomas (Chichester: John Wiley & Sons, Ltd), 290–303,  
887 doi: 10.1002/9781118778371.ch11, 2017.
- 888 Meiners, K.M., Vancoppenolle, M., Thanassekos, S., Dieckmann, G.S., Thomas, D.N., Tison, J.-L.,  
889 Arrigo, A.R., Garrison, D., McMinn, A., Lannuzel, D., van der Merwe, P., Swadling, K., Smith,  
890 W.O. Jr., Melnikov, I. and Raymond, B.: Chlorophyll a in Antarctic sea ice from historical ice core  
891 data, *Geophys. Res., Lett.*, 39, L21602, doi: 10.1029/2012GL053478, 2012.
- 892 Meyer, B., Fuentes, V, Guerra, C., Schmidt, K., Atkinson, A., Spahic, S., Cisewski, B, Freier, U,  
893 Olariaga, A. and Bathmann, U.: Physiology, growth, and development of larval krill *Euphausia*  
894 *superba* in autumn and winter in the Lazarev Sea, Antarctica, *Limnol. Oceanogr.*, 54, 1595-1614,  
895 doi:10.4319/lo.2009.54.5.1595, 2009.
- 896 Meyer, B. et al.: The winter pack-ice zone provides a sheltered but food-poor habitat for larval Antarctic  
897 krill, *Nature Ecol. Evol.*, doi:10.1038/s41559-017-0368-3, 2017.
- 898 Michel, C., Legendre, L., Ingram, R.G., Gosselin, M., and Levasseur, M.: Carbon budget of sea-ice  
899 algae in spring: Evidence of a significant transfer to zooplankton grazers, *J. Geophys. Res.*, 101,  
900 18345-18360, doi:10.1029/96JC00045, 1996.
- 901 Michels, J., Dieckmann, G.S., Thomas, D.N., Schnack-Schiel, S.B., Krell, A., Assmy, P., Kennedy, H.,  
902 Papadimitriou, S., Cisewski, B.: Short-term biogenic particle flux under late spring sea ice in the  
903 western Weddell Sea, *Deep-Sea Res. II*, 55, 1024-1039, doi: 10.1016/j.dsr2.2007.12.019, 2008.
- 904 Montes-Hugo, M., Doney, S.C., Ducklow, H.W., Fraser, W., Martinson, D., Stammerjohn, S.E., and  
905 Schofield, O.: Recent changes in phytoplankton communities associated with rapid regional climate  
906 change along the western Antarctic Peninsula, *Science*, 323, 1470-1473,  
907 doi:10.1126/science.1164533, 2009.
- 908 Moore, J.K., Abbott, M.R., Richman, J.G., Smith, W.O. Jr., Cowles, T.J., Coale, K.H., Gardner, W.D.,  
909 and Barber, R.T.: SeaWiFS satellite ocean colour data at the U.S. Southern Ocean JGOFS line along  
910 170°W, *Geophys. Res. Lett.*, 26, 1465-1468, doi: 10.1029/1999GL900242, 1999.
- 911 Nelson, D.M., Smith, W.O. Jr., Gordon, L.I., and Huber, B.A.: Spring distribution of density, nutrients,  
912 and phytoplankton biomass in the ice edge zone of the Weddell-Scotia Sea, *J. Geophys. Res. Ocean*,  
913 92, 7181-7190, doi: 10.1029/JC092iC07p07181, 1987.
- 914 Patrick, M.R., Smellie, J.L., Harris, A.J.L., Wright, R., Dean, K., Izbekov, P., Garbeil, H., and Pilger,  
915 E.: First recorded eruption of Mount Belinda volcano (Montagu Island), South Sandwich Islands,  
916 *Bull Volcanol*, 67, 415-422, doi: 10.1007/300445-004-0382-6, 2005.



- 917 Park, J., Oh, I-S., Kim, H-C., and Yoo, S.: Variability of SeaWiFs chlorophyll-a in the southwest  
918 Atlantic sector of the Southern Ocean: Strong topography effects and weak seasonality, *Deep-Sea*  
919 *Res. I*, 57, 604-620, doi: 10.1016/j.dsr.2010.01.004, 2010.
- 920 Peck, L.S., Barnes, D.K.A., Cook, A.J., Fleming, A.H., and Clarke, A.: Negative feedback in the cold:  
921 ice retreat produces new carbon sinks in Antarctica, *Global Change Biol.*, 16, 2614-2623, doi:  
922 10.1111/j.1365-2486.2009.02071.x, 2010.
- 923 Perrette, M., Yool, A., Quartly, G.D., and Popova, E.E.: Near-ubiquity of ice-edge blooms in the Arctic,  
924 *Biogeosciences*, 8, 515-524, doi: 10.5194/bg-8-515-2011, 2011.
- 925 Quetin, L. and Ross, R.: Episodic recruitment in Antarctic krill *Euphausia superba* in the Palmer LTER  
926 study region, *Mar. Ecol. Prog. Ser.*, 259, 185-200, doi:10.3354/meps259185, 2003.
- 927 Reid, K. and Croxall, J.P.: Environmental response of upper trophic-level predators reveals a system  
928 change in an Antarctic marine ecosystem, *Proc. R. Soc. Lond. B*, 268, 377-384, doi:  
929 10.1098/rspb.2000.1371, 2001.
- 930 Renaud, P.E., Riedel, A., Michel, C., Morata, N., Gosselin, M., Juul-Pedersen, T., Chiuchiolo, A.:  
931 Seasonal variations in the benthic community oxygen demand: a response to an ice algal bloom in  
932 the Beaufort Sea, *Canadian Arctic. J. Mar. Syst.*, 67, 1-12, doi: 10.1016/j.jmarsys.2006.07.00, 2007.
- 933 Ribeiro, S., Sejr, M.K., Limoges, A., Heikkilä, M., Andersen, T.J., Tallberg, P., Weckström, K.,  
934 Husum, K., Forwick, M., Dalsgaard, T., Massé, G., Seidenkrantz, M.-S., Rysgaard, S., 2017. Sea ice  
935 and primary production proxies in surface sediments from a High Arctic Greenland fjord: spatial  
936 distribution and implications for palaeo-environmental studies. *Ambio* 46 (Suppl. 1), S106–S118.  
937 doi:10.1007/s13280-016-0894-2, 2017.
- 938 Riebesell, U., Schloss, I., and Smetacek, V.: Aggregation of algae released from melting sea ice:  
939 implications for seeding and sedimentation, *Polar Biol.*, 11, 239-248, 1991.
- 940 Ross, R.M., Quetin, L.B., Baker, K.S., Vernet, M., and Smith, R.C.: Growth limitation in young  
941 *Euphausia superba* under field conditions. *Limnol. Oceanogr.*, 45, 31-43, doi:  
942 10.4319/lo.2000.45.1.0031, 2000.
- 943 Roukaerts, A., Cavagna, A-J., Fripiat, F., Lannuzel, D., Meiners, K.M., and Dehairs, F.: Sea-ice algal  
944 primary production and nitrogen uptake off East Antarctica, *Deep-Sea Res. II*, 131, 140-149, doi:  
945 10.1016/j.dsr2.2015.08.007, 2016.
- 946 Ryabov, A.B., de Ross, A.M., Meyer, B., Kawaguchi, S., and Blasius, B.: Competition-induced  
947 starvation drives large-scale population cycles in Antarctic krill, *Nat. Ecol. Evol.*, 1, 0177, doi:  
948 10.1038/s41559-017-0177, 2017.



- 949 Saba, G.K., Fraser, W.R., Saba, V.S., Iannuzzi, R.A., Coleman, K.E., Doney, S.C., Ducklow, H.W.,  
950 Martinson, D.G., Miles, T.N., Patterson-Fraser, D.L., Stammerjohn, S.E., Steinberg, D.K., and  
951 Schofield, O.M.: Winter and spring controls on the summer food web of the coastal West Antarctic  
952 Peninsula, *Nat. Comms.*, 5, 4318, doi:10.1038/ncomms5318, 2014.
- 953 Schallenberg, C., van der Merwe, P., Chever, F., Cullen, J.T., Lannuzel, D., and Bowie, A.R.: Dissolved  
954 iron and iron(II) distributions beneath the pack ice in the East Antarctic (120°E) during the  
955 winter/spring transition, *Deep-Sea Res. II*, 131, 96-110, doi: 10.1016/j.dsr2.2015.02.019, 2015.
- 956 Schlitzer, R.: Ocean Data View <http://odv.awi.de> (2017).
- 957 Schmidt, K., and Atkinson, A.: Feeding and food processing in Antarctic krill (*Euphausia superba*  
958 Dana), in V. Siegel (ed.), *Biology and Ecology of Antarctic krill*, *Adv. Polar Ecol.*,  
959 doi:10.1007/978-3-319-29279-3\_5, 2016.
- 960 Schmidt, K., Atkinson, A., Petzke, K.J., Voss, M. and Pond, D.W.: Protozoans as a food source for  
961 Antarctic krill, *Euphausia superba*: complementary insights from stomach content, fatty acids, and  
962 stable isotopes, *Limnol. Oceanogr.*, 51, 2409-2427, doi: 10.4319/lo.2006.51.5.2409, 2006.
- 963 Schmidt, K., Atkinson, A., Steigenberger, S., Fielding, S., Lindsay, M.C.M., Pond, D.W., Tarling, G.A.,  
964 Klevjer, T.A., Allen, C.S., Nicol, S., and Achterberg, E.P.: Seabed foraging by Antarctic krill:  
965 Implications for stock assessment, benthic-pelagic coupling and the vertical transfer of iron, *Limnol.*  
966 *Oceanogr.*, 56, 1411-1428, doi: 10.4319/lo.2011.56.4.1411, 2011.
- 967 Schmidt, K., Atkinson, A., Venables, H.J., and Pond, D.W.: Early spawning of Antarctic krill in the  
968 Scotia Sea is fuelled by 'superfluous' feeding on non-ice associated phytoplankton blooms. *Deep-*  
969 *Sea Res. II*, 59-60, 159-172, doi: 10.1016/j.dsr2.2011.05002, 2012.
- 970 Schmidt, K., Atkinson, A., Pond, D.W., and Ireland, L.C.: Feeding and overwintering of Antarctic krill  
971 across its major habitats: The role of sea ice cover, water depth, and phytoplankton abundance,  
972 *Limnol. Oceanogr.*, 59, 17-36, doi: 10.4319/lo.2014.59.1.0017, 2014.
- 973 Schmidt, K., Schlosser, C., Atkinson, A., Fielding, S., Venables, H.J., Waluda, C.M., and Achterberg,  
974 E.P.: Zooplankton gut passage mobilizes lithogenic iron for ocean productivity, *Current Biol*, 26, 1-  
975 7, doi: 10.1016/j.cub.2016.07.058, 2016.
- 976 Smetacek, V. and Nicol, S.: Polar ocean ecosystems in a changing world, *Nature*, 437, 363-368,  
977 doi:10.1038/nature04161, 2005.
- 978 Smik, L., Belt, S.T., Lieser, J.L., Armand, L.K., and Leventer, A.: Distributions of highly branched  
979 isoprenoid alkenes and other algal lipids in surface waters from East Antarctica: Further insights for  
980 biomarker-based paleo sea-ice reconstruction. *Org. Geochem.*, 95, 71-80, doi:  
981 10.1016/j.orggeochem.2016.02.011, 2016.



- 982 Smith, W.O., Jr., and Nelson, D.M.: The importance of ice-edge blooms in the Southern Ocean,  
983 *Biosciences*, 36, 251-257, doi: 10.2307/1310215, 1986.
- 984 Smith, W.O., Jr., Shields, A.R., Peloquin, J.A., Catalano, G., Tozzi, S., Dinniman, M.S., and Asper,  
985 V.A., Biogeochemical budgets in the Ross Sea: Variations among years, *Deep-Sea Res. II*, 53, 815-  
986 833, doi: 10.1016/j.dsr2.2006.02.014, 2006.
- 987 Søreide, J.E., Leu, E., Berge, J., Graeve, M., and Falk-Petersen, S.: Timing of blooms, algal food  
988 quality and *Calanus glacialis* reproduction and growth in a changing Arctic, *Glob. Change Biol.* 16,  
989 3154-3163, doi: 10.1111/j.1365-2486.2010.02175.x, 2010.
- 990 Spreen, G., Kaleschke, L., and Heygster, G.: Sea ice remote sensing using AMSR-E 89 GHz channels,  
991 *J. Geophys. Res.*, 113, C02S03, doi:10.1029/2005JC003384, 2008.
- 992 Stammerjohn, S., Massom, R., Rind, D., and Martinson, D.: Regions of rapid sea ice change: An inter-  
993 hemispheric seasonal comparison, *Geophys. Res. Lett.*, 39, L06501, doi:10.1029/2012GL050874,  
994 2012.
- 995 Stammerjohn, S., and Maksym, T.: Gaining (and losing) Antarctic sea ice: variability, trends and  
996 mechanisms, In: 'Sea Ice', ed. D. N. Thomas (Chichester: John Wiley & Sons, Ltd), 261–289,  
997 doi: 10.1002/9781118778371.ch10, 2017.
- 998 Sullivan, C.W., McClain, C.R., Comiso, J.C., and Smith, W.O. Jr., Phytoplankton standing crops within  
999 an Antarctic ice edge, *J. Geophys. Res.*, 93, 12487-12498, doi: 10.1029/JC093iC10p12487, 1988.
- 1000 Tréguer, P., and Jacques, G.: Dynamics of nutrients and phytoplankton, and fluxes of carbon, nitrogen  
1001 and silicon in the Antarctic Ocean. *Polar Biol.*, 12, 149-169, 1992.
- 1002 Trivelpiece, W., Hinke, J., Miller, A., Reiss, C., Trivelpiece, S., Watters, G.: Variability in krill biomass  
1003 links harvesting and climate warming to penguin population changes in Antarctica. *Proc. Nat. Acad.*  
1004 *Sc. Unit. St. Am.*, 108, 7625-7628, doi:10.1073/pnas.1016560108, 2011.
- 1005 Vancoppenolle, M., Meiners, K.M., Michel, C., Bopp, L., Brabant, F., Carbat, G., Delille, B., Lannuzel,  
1006 D., Madec, G., Moreau, S., Tison, J-L., and van der Merwe, P.: Role of sea ice in global  
1007 biogeochemical cycles: emerging views and challenges, *Quat. Sci. Rev.*, 79, 207-230,  
1008 doi:10.1016/j.quascirev.2013.04.011, 2013.
- 1009 Venables, H.J., Clarke, A., Meredith, M.P.: Wintertime controls on summer stratification and  
1010 productivity at the western Antarctic Peninsula, *Limnol. Oceanogr.*, 58, 1035-1047, doi:  
1011 10.4319/lo.2013.58.1035, 2013.
- 1012 Wang, S.W., Budge, S.M., Gradinger, R.R., Iken, K., and Wooller, M.J., Fatty acid and stable isotope  
1013 characteristics of sea ice and pelagic particulate organic matter in the Bering Sea: tools for



1014       estimating sea ice algal contribution to Arctic food web production, *Oecolog.*, 174, 699-712,  
1015       doi:10.1007/s00442-013-2832-3, 2014.

1016       Wang, S.W., Budge, S.M., Iken, K., Gradinger, R.R., Springer, A.M., and Wooller, M.J., Importance of  
1017       sympagic production to Bering Sea zooplankton as revealed from fatty acid-carbon stable isotope  
1018       analyses, *Mar. Ecol. Prog. Ser.*, 518, 31-50, doi:10.3354/meps11076, 2015.

1019       Ward, P., Shreeve, R., Atkinson, K., Korb, R., Whitehouse, M., Thorpe, S., Pond, D., and Cunningham,  
1020       N.: Plankton community structure and variability in the Scotia Sea: austral summer 2003, *Mar. Ecol.*  
1021       *Prog. Ser.*, 309, 75-91, doi:10.3354/meps309075, 2006.

1022       Wassmann, P., Duarte, C.M., Agusti, S., and Sejr, M.K.: Footprints of climate change in the Arctic  
1023       marine ecosystem, *Glob. Change Biol.*, 17, 1235-1249, doi: 10.1111/j.1365-2486.2010.02311.x,  
1024       2011.

1025

1026

1027

1028

1029

1030

1031

1032

1033

1034

1035

1036

1037

1038



1039 **Table 1.** *Euphausia superba*: carbon isotopic signature ( $\delta^{13}\text{C}$ ) of IPSO<sub>25</sub> and HBI III extracted from ~30  
 1040 pooled, whole krill (mean  $\pm$  SD, n=3) at four stations.

	Stn 5	Stn 17	Stn 31	Stn 47	Mean
$\delta^{13}\text{C}$ - IPSO <sub>25</sub> (‰)	-15.75 $\pm$ 0.15	-12.63 $\pm$ 0.15	-9.21 $\pm$ 0.02	-	-12.53 $\pm$ 3.27
$\delta^{13}\text{C}$ - HBI III (‰)	-42.54 $\pm$ 0.27	-	-39.09 $\pm$ 0.16	-45.05 $\pm$ 0.07	-42.23 $\pm$ 2.44

1041

1042

1043

1044

1045 **Table 2.** *Euphausia superba*: concentrations of IPSO<sub>25</sub> and HBI III in different body fractions. Average  
 1046 stomach values are used as baseline for comparisons across body fractions, 'Ratio (stomach/X)'. X –  
 1047 digestive gland, gut, muscle, rest or whole krill. The I/(I+H) ratio was calculated as the ratio of means  
 1048 for those stations where both IPSO<sub>25</sub> and HBI III had been detected in at least one of the body fractions.  
 1049 r - range

	IPSO <sub>25</sub>			HBI III			I/(I+H)
	Mean ( $\pm$ SD) (ng g <sup>-1</sup> )	Maximum (ng g <sup>-1</sup> )	Ratio (stomach/X)	Mean ( $\pm$ SD) (ng g <sup>-1</sup> )	Maximum (ng g <sup>-1</sup> )	Ratio (stomach/X)	Ratio of Means r: 0.00-0.95
Stomach	2875 $\pm$ 5277	14337		14358 $\pm$ 18844	58902		0.17 r: 0.00-0.95
Digestive gland	958 $\pm$ 1609	4523	3	5018 $\pm$ 6043	19686	3	0.16 r: 0.00-0.92
Gut	812 $\pm$ 1414	3601	3.5	52027 $\pm$ 167732	584461	0.3	0.02 r: 0.00-0.91
Muscle	51 $\pm$ 46	125	56	245 $\pm$ 238	861	59	0.17 r: 0.01-0.51
Rest	188 $\pm$ 160	387	15	804 $\pm$ 731	2340	18	0.19 r: 0.00-0.62
Whole krill	219 $\pm$ 222	618	13	1393 $\pm$ 1638	3221	10	0.14 r: 0.00-0.73
Pellets	1549 $\pm$ 379	1973		1263 $\pm$ 410	4419		

1050

1051 Analysed stations (IPSO<sub>25</sub>): Stn 5, 10, 13, 14, 17, 22, 31, 34, 54

1052 Analysed stations (HBI III): Stn 5, 10, 13, 14, 17, 22, 31, 34, 47, 54, 60

1053 Analysed stations [I/(I+H)]: Stn 5, 10, 13, 14, 17, 22, 31, 34, 54

1054 Analysed stations, pellets (IPSO<sub>25</sub>): Stn 21, 32

1055 Analysed stations, pellets (HBI III): Stn 9, 10, 15, 21, 31, 32, 34, 42, 45, 47, 52, 54, 60, 61

1056

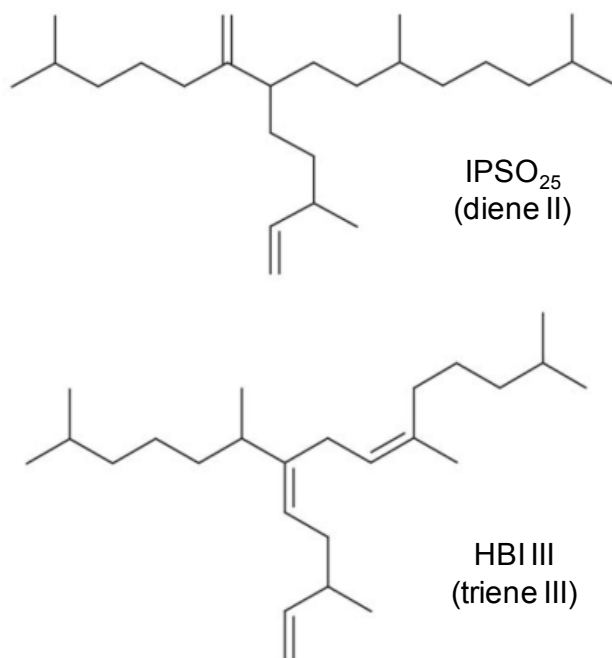


**Fig. 1**

1057

1058

1059 **Fig. 1.** Chemical structures of diatom highly branched isoprenoid (HBI) biomarkers described in this  
1060 study.

1061

1062

1063

1064

1065

1066

1067

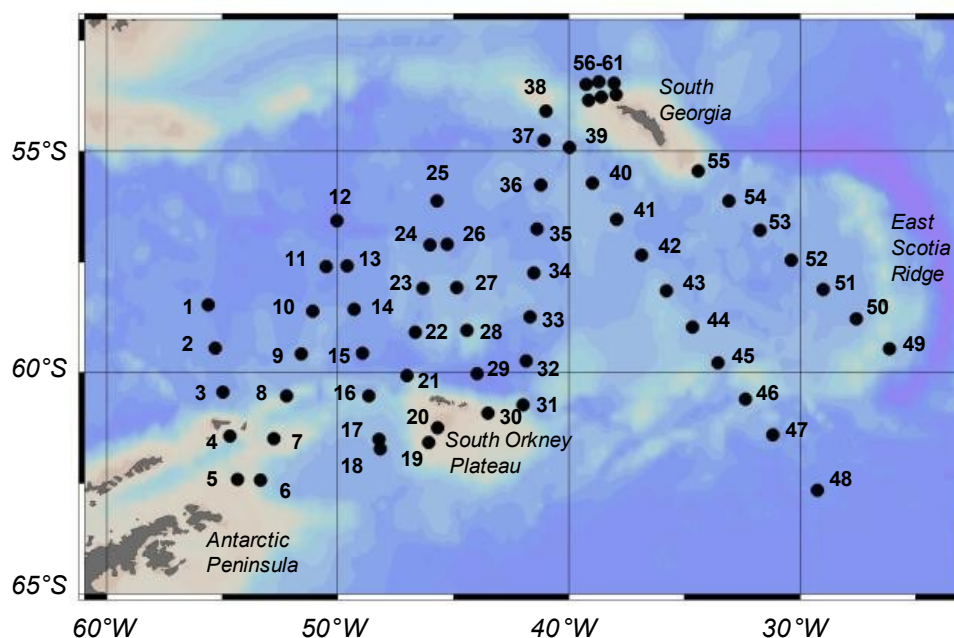


**Fig. 2**

1068

1069

1070 **Fig. 2.** Scotia Sea and South Georgia: sampling locations during austral summer 2003. The date of  
1071 sampling progressed from January, 9<sup>th</sup> (Station 1) to February 16<sup>th</sup> (Station 61). Shelf areas ( $\leq 1000$  m)  
1072 are presented in light brown colour.

1073

1074

1075

1076

1077

1078

1079

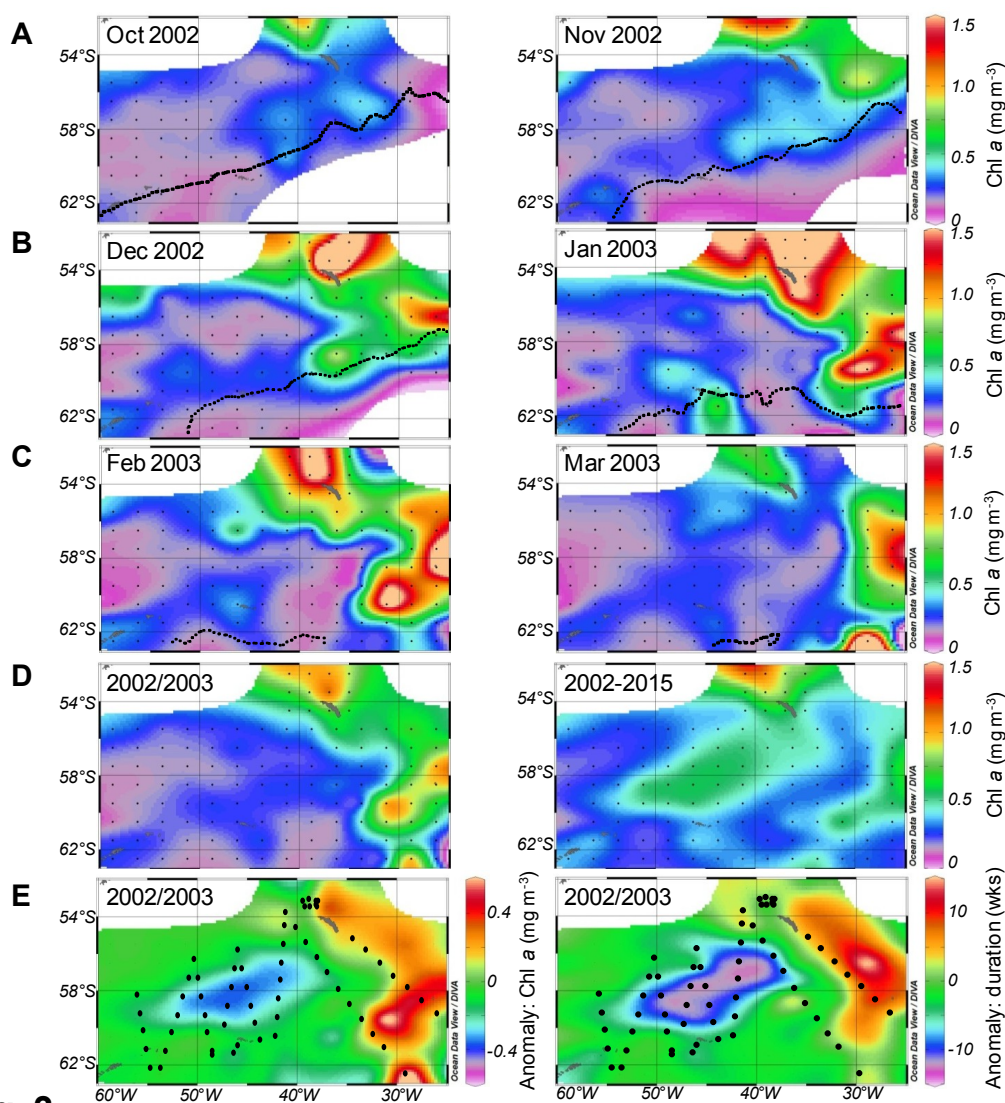


**Fig. 3**

1080

1081 **Fig. 3.** Phytoplankton bloom development in the Scotia Sea in 2002/2003 and on a longer-term average  
 1082 (2002-2015). Chl *a* concentrations in the **A**) early season (L: Oct. 2002; R: Nov. 2002), **B**) mid-season  
 1083 (L: Dec. 2002; R: Jan. 2003) and **C**) late season (L: Feb. 2003; R: Mar. 2003). **D**) Average annual chl *a*  
 1084 concentrations, Sept-Mar (L: 2002/2003; R: 2002-2015). **E**) Anomaly in 2002/2003 (Sept.–Mar.)  
 1085 compared to the longer-term average, 2002-2015 (L: chl *a* concentration; R: bloom duration). Chl *a*  
 1086 concentrations were derived from ocean colour radiometry (MODIS, 8-day composites). A bloom was



1087 defined as  $>0.5 \text{ mg Chl } a \text{ m}^{-3}$ . The dashed line represents the mean position of the 15% ice edge during  
1088 each of the months. In panels E, the position of our sampling stations is given.

1089

1090

1091

1092

1093

1094

1095

1096

1097

1098

1099

1100

1101

1102

1103

1104

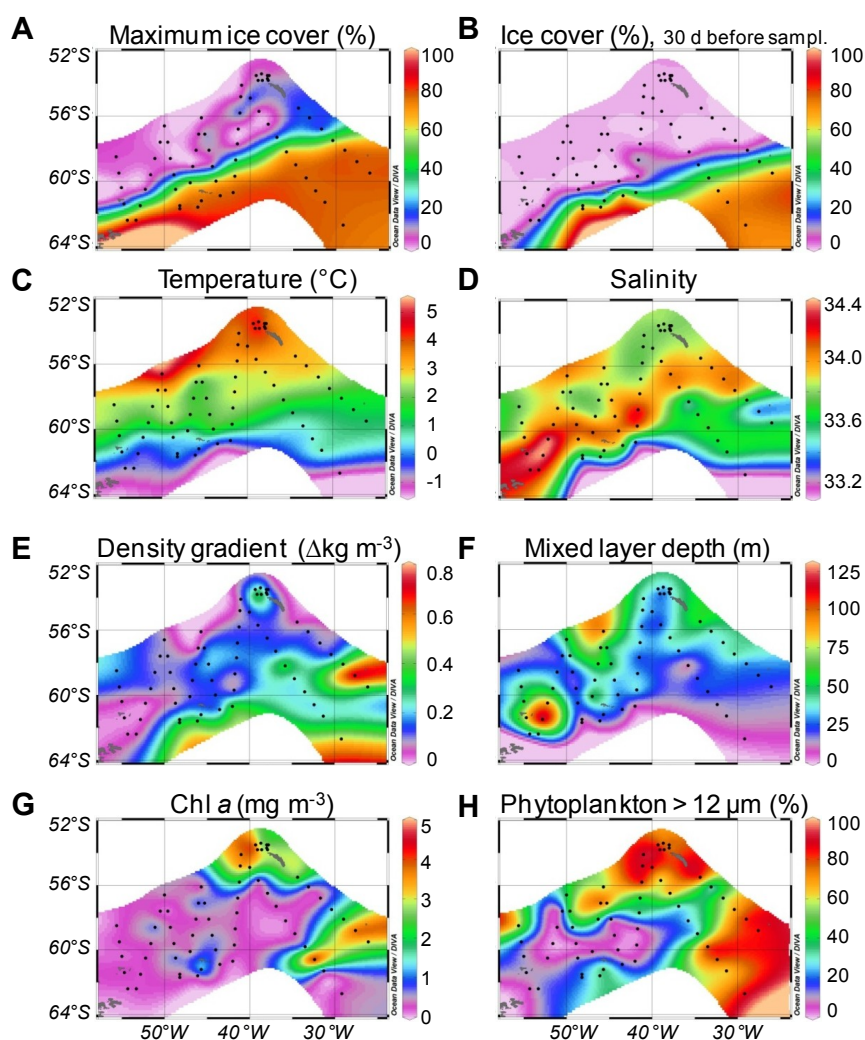
1105

1106

1107

1108

1109

**Fig. 4**

1110

1111 **Fig. 4.** Oceanographic data: **A)** Maximum ice cover within the 2002/2003 season. **B)** Ice cover 30 days  
1112 before each station was sampled. **C)** Surface temperature, **D)** Surface salinity, **E)** Maximum density  
1113 gradient per 10 m water column, **F)** Mixed layer depth, **G)** Total chlorophyll *a* (Chl *a*) concentration of  
1114 cells >0.2  $\mu\text{m}$ , **H)** Proportion of large phytoplankton (>12  $\mu\text{m}$ ) based on size-fractionated Chl *a*  
1115 measurements (% of total Chl *a*).

1116

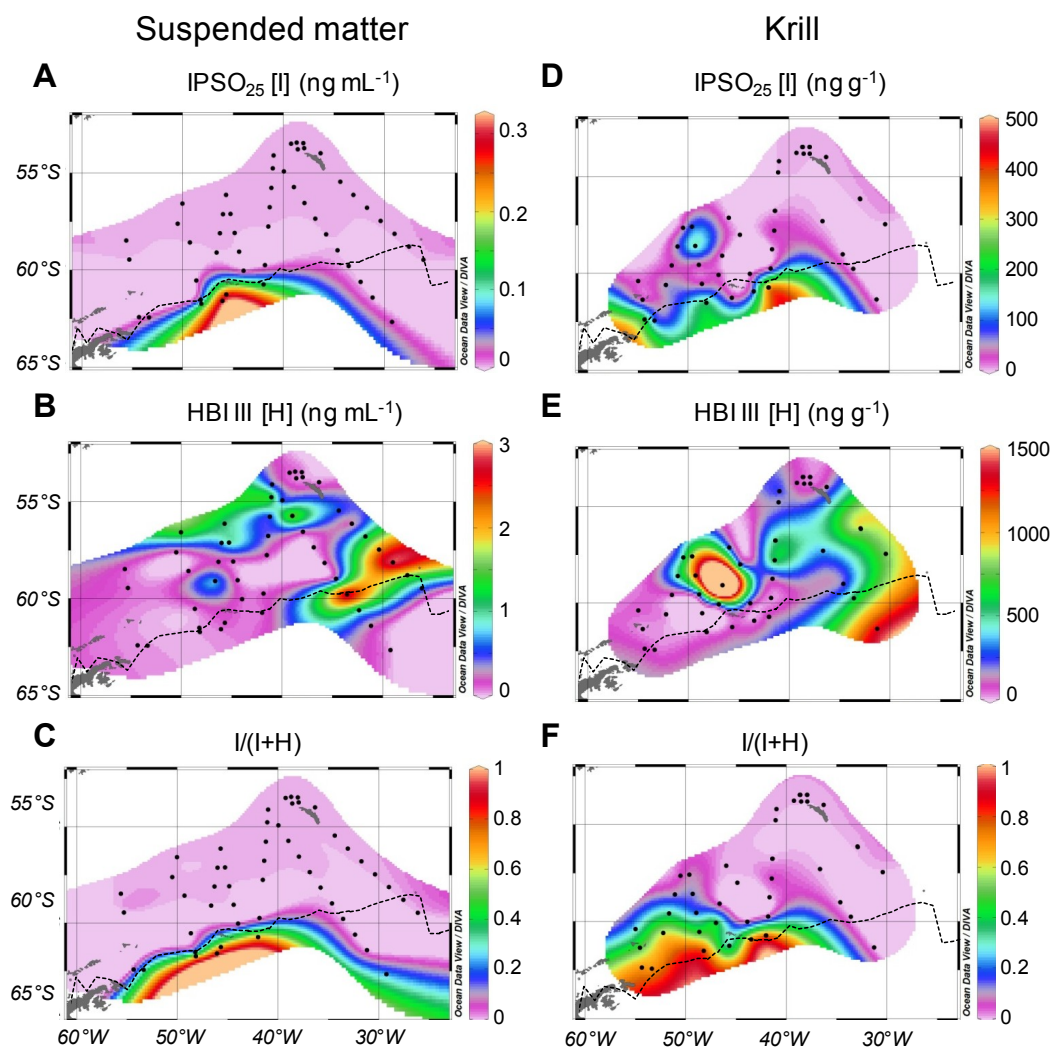


**Fig. 5**

1117

1118 **Fig. 5.** Highly branched isoprenoid (HBI) concentrations in suspended matter from surface waters (left)  
1119 and whole krill (right): **A, D**) IPSO<sub>25</sub> concentrations. **B, E**) HBI III concentrations. **C, F**) IPSO<sub>25</sub> vs HBI  
1120 III ratios. The dashed line represents the mean position of the 15% ice edge during January.

1121

1122

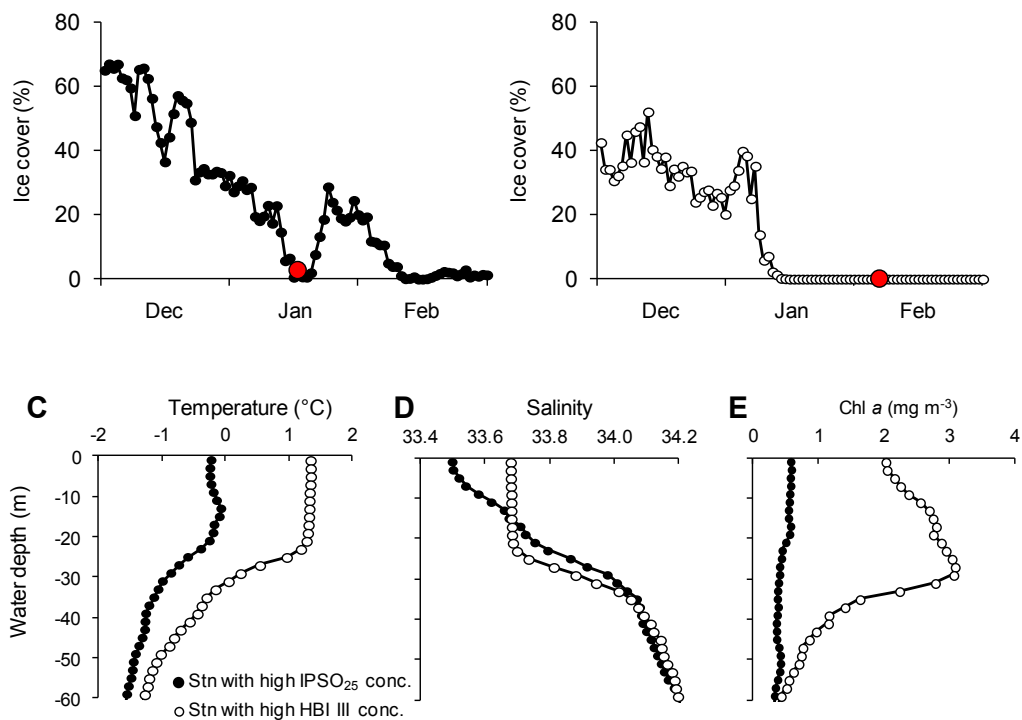


**Fig. 6**

1123

1124 **Fig. 6.** Oceanographic differences between stations with high IPSO<sub>25</sub> vs. high HBI III concentrations in  
 1125 suspended matter. **A)** Time line of sea ice cover at stations with high IPSO<sub>25</sub> concentrations (mean of  
 1126 Stn 18, 19, 20, 31). The red dot indicates the time of sampling. **B)** Time line of sea ice cover at stations  
 1127 with high HBI III concentrations (mean of Stn 45, 50, 51, 52). **C)** Vertical profiles of temperature, **D)**  
 1128 salinity and **E)** chlorophyll *a*.

1129

1130

1131

1132

1133

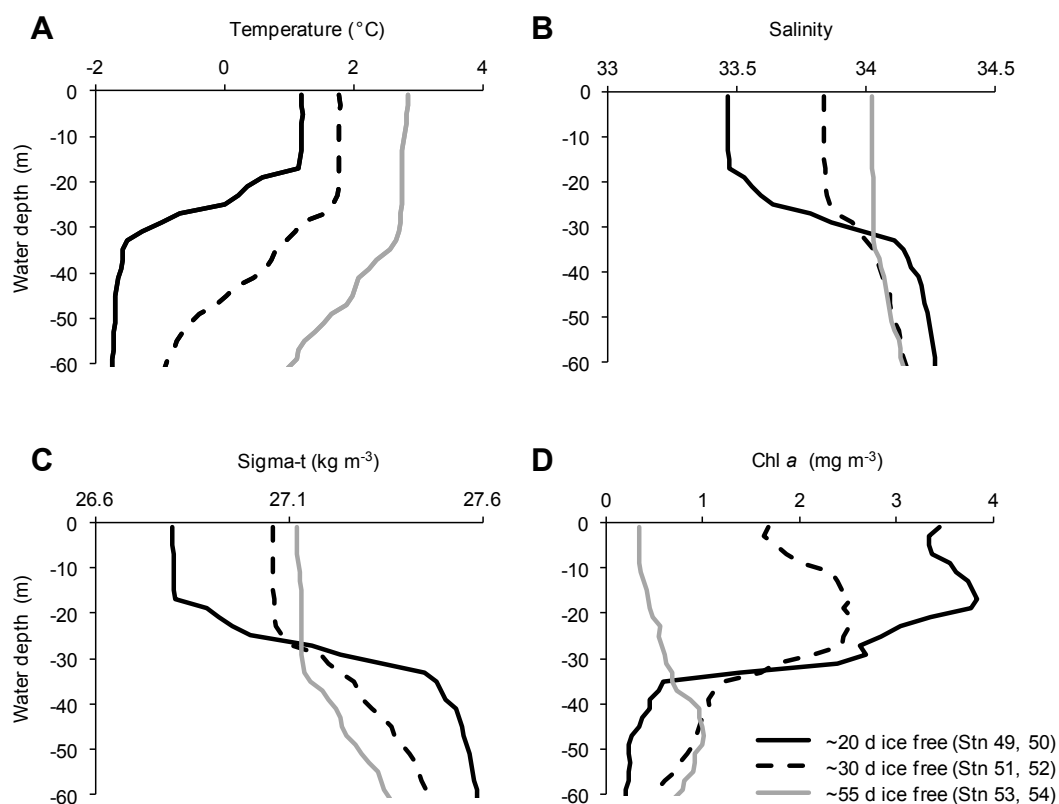


**Fig. 7**

1134

1135 **Fig. 7.** Oceanographic characteristics along the gradient in HBI III concentrations in the eastern Scotia  
1136 Sea. **A)** Vertical profiles of temperature, **B)** salinity, **C)** density and **D)** chl *a* for the mean of two  
1137 neighbouring stations. The HBI III content of the suspended matter was highest at stations which had  
1138 been ice free for ~30 days ( $3.4 \pm 0.6 \text{ ng mL}^{-1}$ , Stn 51 & 52), but lower for stations that had become ice  
1139 free more recently ( $1.3 \pm 0.9 \text{ ng mL}^{-1}$ , Stn 49 & 50) or longer ago ( $0.9 \pm 1.0 \text{ ng mL}^{-1}$ , Stn 53 & 54).

1140

1141

1142

1143

1144

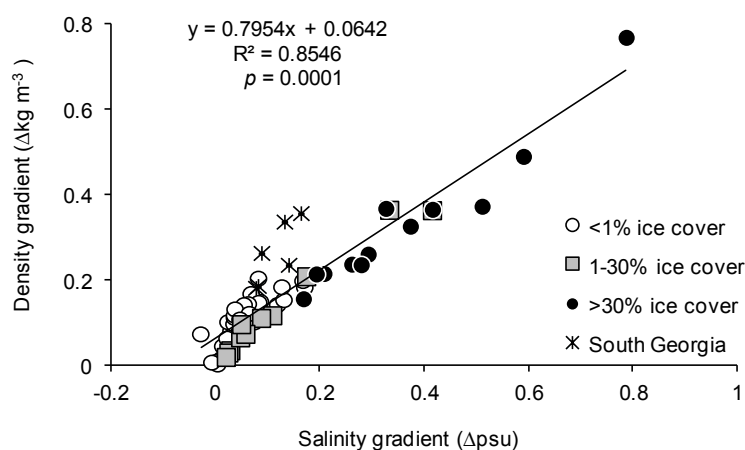


**Fig. 8**

1145

1146

1147 **Fig. 8.** The role of seasonal ice melt for water column stratification. During spring 2003, the maximum  
 1148 density gradient per 10 m water column was a linear function of the co-occurring salinity gradient, with  
 1149 strongest density gradients at stations that had been ice covered by >30% one month before sampling.  
 1150 The remaining variability in the density gradient is explained by temperature (GLM: density gradient =  
 1151  $0.00254 + 0.7255 \text{ salinity gradient} + 0.07828 \text{ temperature gradient}$ ;  $R^2 = 0.9889$ ).

1152

1153

1154

1155

1156

1157

1158

1159

1160

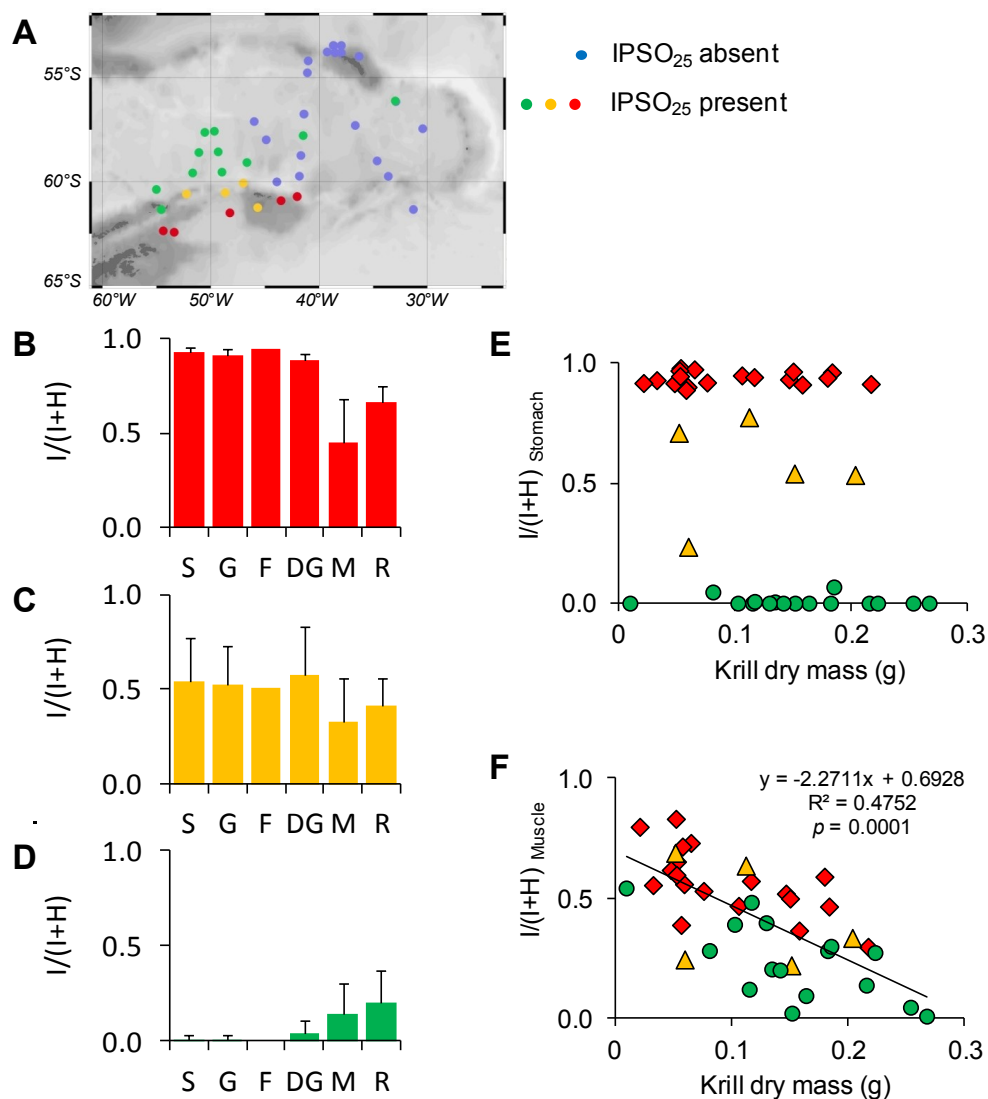


**Fig. 9**

1161

1162 **Fig. 9.** *E. superba*: multiple scenarios of krill feeding history on ice diatoms. **A)** Location of stations  
 1163 where IPSO<sub>25</sub> was present in krill (red – Scenario 1, amber – Scenario 2, green – Scenario 3) or absent  
 1164 (blue). **B)** Scenario 1: Krill are mainly feeding on ice diatoms.  $I/(I+H)$  ratios are high (>0.9) in stomach  
 1165 (S), gut (G), faecal pellets (F) and digestive gland (DG), but lower (0.4-0.7) in muscles (M) and rest of  
 1166 the body (R). **C)** Scenario 2: Krill are feeding on a mixture of ice diatoms and open water diatoms.  
 1167  $I/(I+H)$  ratios are moderate (~0.5) in stomach, gut, faecal pellets and digestive gland, but lower (0.3-0.4)



1168 in muscles and rest of the body. **D)** Scenario 3: Krill are feeding on open water diatoms, but fed on ice  
1169 diatoms in the past.  $I/(I+H)$  ratios are very low ( $<0.1$ ) in stomach, gut and digestive gland, but higher  
1170 ( $0.1-0.2$ ) in muscles and rest of the body. **E, F)** The effect of krill body size on their feeding on ice  
1171 diatoms.  $I/(I+H)$  ratios are presented separately for krill stomach content and muscle. Colour of symbols  
1172 in accordance with panels B-D: Red – krill that fed currently on ice diatoms, yellow – krill that fed  
1173 currently on a mixture of ice- and open water diatoms, green – krill that fed currently on open water  
1174 diatoms. Individuals ranged from 16-42 mm in standard body length [L] and 0.01-0.27 g in dry mass  
1175 [M] ( $M = 1 \cdot 10^{-6} L^{3.2452}$ ,  $R^2 = 0.9707$ ). Each symbol represents 3-15 pooled individuals of the same body  
1176 length.

1177

1178

1179

1180

1181

1182

1183

1184

1185

1186

1187

1188

1189

1190

1191

1192

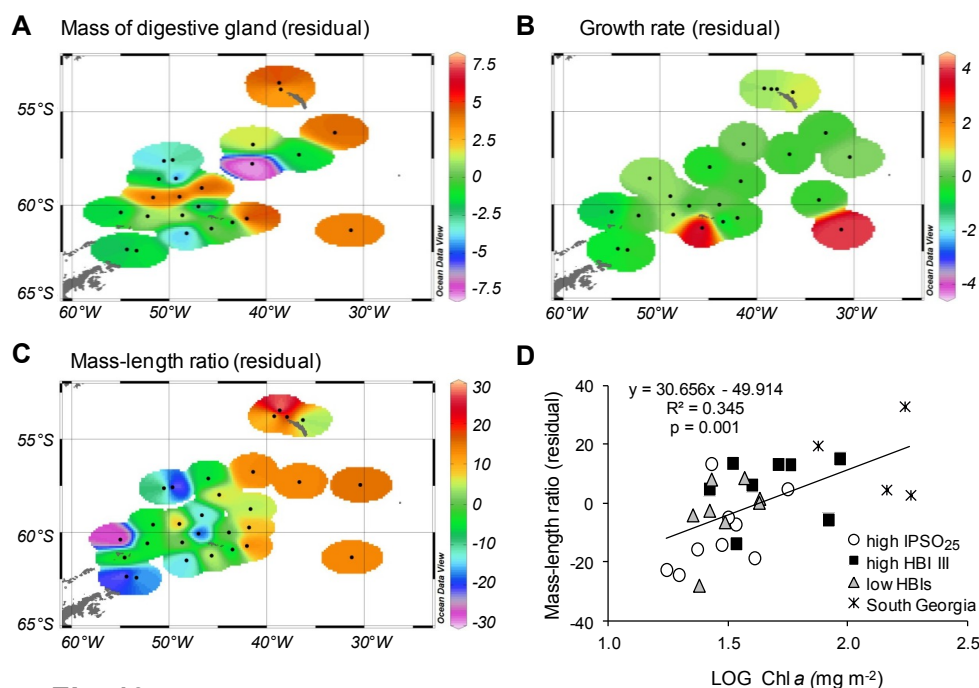


**Fig. 10**

1193

1194

1195 **Fig. 10.** *E. superba*: local differences in krill body conditions as indicated by the size of their digestive  
 1196 gland, their growth rate or mass-length ratio. To account for differences in krill body length, residuals  
 1197 rather than absolute values are presented. Residuals were calculated as positive or negative deviations  
 1198 from the relationship between the index of body condition (y) and krill length (x). Positive values denote  
 1199 ‘above-average’ body conditions for their size, negative values suggest ‘below-average’ body conditions.  
 1200 **A)** Mass of the digestive gland.  $y = 85.234x + 2.5386$ ;  $R^2 = 0.7271$ ,  $n = 25$ . **B)** Krill growth rate in mass,  
 1201 based on original data from Atkinson et al. (2006).  $y = 65586x^{-3.069}$ ;  $R^2 = 0.3265$ ,  $n = 24$ . **C)** Krill mass-  
 1202 length ratio.  $y = 0.0016x^{3.2479}$ ,  $R^2 = 0.8627$ ,  $n = 29$ . **D)** Linear regression between the residuals of krill  
 1203 mass-length ratio (panel C) and the availability of food, indicated by the integrated chl *a* concentration in  
 1204 the upper 100 m-water column. Krill from different locations are distinguished by their IPSO<sub>25</sub>- or HBI  
 1205 III content: ‘high IPSO<sub>25</sub>’ (>30 ng g<sup>-1</sup>), ‘high HBI III’ (>100 ng g<sup>-1</sup>), ‘low IPSO<sub>25</sub> and HBI III’ (< 100 ng  
 1206 g<sup>-1</sup>), ‘South Georgia’ (< 100 ng g<sup>-1</sup>). Each symbol represents 3-15 pooled individuals of the same body  
 1207 length.

1208

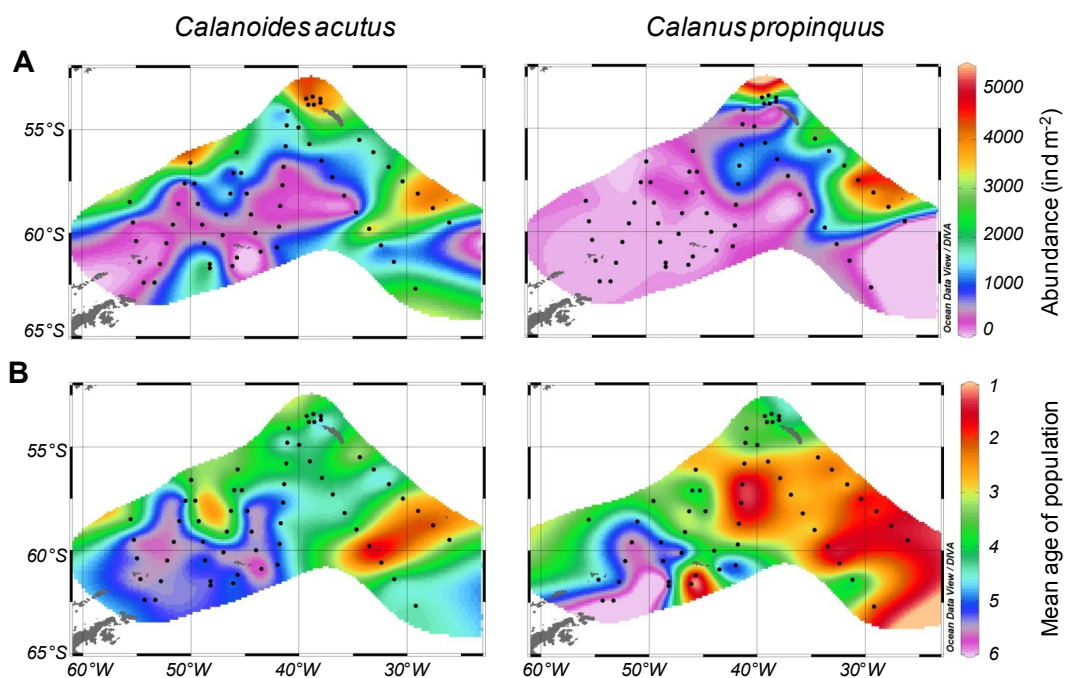


**Fig. 11**

1209

1210

1211 **Fig. 11.** Large calanoid copepods, *Calanoides acutus* and *Calanus propinquus*. **A)** Species abundance

1212 and **B)** mean age of the population. Six copepodite stages of increasing age were considered: 1<sup>st</sup>, 2<sup>nd</sup>,

1213 3<sup>rd</sup>, 4<sup>th</sup>, 5<sup>th</sup> and 6<sup>th</sup>. Low numbers indicate a young age of the population, dominant by new recruits

1214 (stage 1-3). Late copepodite stages (stage 5-6) represent the old, overwintered generation.

1215

1216

1217